universität wien

MASTERARBEIT | MASTER'S THESIS

Titel | Title

Microbial consortia potentially couple thiosulfate oxidation with the reduction of iron(III) oxides

verfasst von | submitted by

Dott. Nicola Battisti

angestrebter akademischer Grad | in partial fulfilment of the requirements for the degree of

Master of Science (MSc)

Wien | Vienna, 2025

Studienkennzahl lt. Studienblatt | Degree programme code as it appears on the student record sheet:	UA 066 830
Studienrichtung lt. Studienblatt | Degree programme as it appears on the student record sheet:	Masterstudium Molecular Microbiology, Microbial Ecology and Immunobiology
Betreut von | Supervisor:	Univ.-Prof. Dipl.-Biol. Dr. Alexander Loy

Abstract

The microbial sulfur cycle is a crucial biogeochemical process in wetland ecosystems, playing a significant role in regulating organic carbon decomposition and methane emissions. Despite the relatively small standing pool of sulfate, efficient sulfur recycling facilitates rapid sulfate renewal, supporting sulfate reduction rates comparable to those observed in marine sediments. However, the mechanisms underlying sulfur oxidation in wetland ecosystems remain poorly understood. It has been hypothesized that iron(III) minerals may be directly involved in driving the microbial sulfur oxidation, but this hypothesis has yet to be explored experimentally. In this thesis, we leveraged an enrichment culture derived from peatland to investigate the potential role of ferrihydrite in driving the oxidation of thiosulfate, one of key intermediates in the oxidative sulfur cycle in the freshwater ecosystem. Our experiments integrated both a chemical analysis and microbial ecology approaches to understand the stoichiometry and key microbial members underlying the ferrihydrite-coupled thiosulfate oxidation process. Our findings suggest members of the consortia are able to use intermediate sulfur compounds and iron(III) oxides to fix inorganic carbon, and support the rest of the community. We propose potential scenarios allowing the coupled redox reactions and the growth of the culture. Furthermore, this work underlines the intricate interactions between members of the enrichment culture, indicating the potential involvement of cooperative growth of the community members.

Zusammenfassung

Der mikrobielle Schwefelkreislauf ist ein entscheidender biogeochemischer Prozess in Feuchtgebiet-Ökosystemen und spielt eine bedeutende Rolle bei der Regulierung des Abbaus organischen Kohlenstoffs sowie der Methanemissionen. Trotz des relativ kleinen verfügbaren Sulfatpools ermöglicht ein effizienter Schwefelkreislauf eine schnelle Sulfatregeneration und unterstützt Sulfatreduktionsraten, die mit denen in marinen Sedimenten vergleichbar sind. Dennoch sind die zugrunde liegenden Mechanismen der Schwefeloxidation in Feuchtgebieten noch unzureichend verstanden. Es wurde die Hypothese aufgestellt, dass Eisen(III)-Minerale direkt an der mikrobiellen Schwefeloxidation beteiligt sein könnten, doch diese Hypothese wurde bislang nicht experimentell untersucht. In dieser Arbeit haben wir eine aus einem Torfmoor gewonnene Anreicherungskultur genutzt, um die potenzielle Rolle von Ferrihydrit bei der Oxidation von Thiosulfat zu untersuchen – einem der wichtigsten Intermediate im oxidativen Schwefelkreislauf von Süßwasserökosystemen. Unsere Experimente kombinierten chemische Analysen und mikroökologische Ansätze, um die Stöchiometrie und die zentralen mikrobiellen Akteure des Ferrihydrit-gekoppelten Thiosulfat-Oxidationsprozesses zu verstehen. Unsere Ergebnisse deuten darauf hin, dass Mitglieder des Konsortiums in der Lage sind, intermediäre Schwefelverbindungen und Eisen(III)-Oxide zu nutzen, um anorganischen Kohlenstoff zu fixieren und den Rest der Gemeinschaft zu unterstützen. Wir schlagen mögliche Szenarien vor, die gekoppelte Redoxreaktionen und das Wachstum der Kultur ermöglichen. Darüber hinaus hebt diese Arbeit die komplexen Wechselwirkungen zwischen den Mitgliedern der Anreicherungskultur hervor und weist auf eine mögliche kooperative Wachstumsstrategie innerhalb der Gemeinschaft hin.

Table of content

Abstract.....2
Zusammenfassung.....2
Table of content.....3
Introduction.....4
Material and methods.....10
Sediment samples, enrichment and cultivation.....10
Experimental designs.....10
Analytic measurement.....12
Fluorescence microscopy.....14
Community analysis.....14
Reagents preparations.....16
Results.....17
Thiosulfate stability in freshwater media.....17
Thiosulfate oxidation coupled with iron reduction.....18
Gas chromatography.....22
Fluorescence microscopy.....23
DNA extraction yields.....24
Community profiling.....25
Discussion.....27
Conclusion.....34
Acknowledgement.....35
Reference.....36

Introduction

Peatlands are a category of freshwater wetlands characterized by an anaerobic waterlogged environment that slows down the decomposition of the organic matter, forming the accumulation of layers of partially undecomposed organic matter (peat) (Charman, 2009; Jaszczuk et al, 2024). The majority of peatlands, accounting for the 80 % of the total, are located in the northern hemisphere (Limpens et al., 2008). These northern peatlands, even if they only cover 3 % of the earth drylands, store between 530 and 694 Gt of organic carbon (C), accounting for almost the 21 % of the total organic C stored in the soil worldwide (Yu et al., 2010; Gallego-Sala et al., 2018; Leifeld and Menichetti, 2018). The turnover of this large stock of carbon is influenced by the cycling of iron (Fe) and sulfur (S). Fe is responsible both of the stability of the dissolved organic matter (DOM), as consequences of the formation of Fe-DOM aggregate, and mineralization of the DOM, as consequence of microbial dissimilatory iron reduction metabolism (Kügler et al., 2019; Chen et al., 2020; Song et al., 2022; Curtinrich et al., 2024). While S compounds, such as sulfate, can serve as an alternative terminal electron acceptor for microbial degradation of organic carbon compounds , diverting the electron flow from methanogenesis to microbial sulfur reduction (Boothroyd et al., 2021). The interconnection among these cycling processes is of most interests considering its direct impact on the retention of organic carbon, and the emission of greenhouse gasses such methane (CH_4) and nitrous oxide (N_2O), created as results of the carbon cycling (Frolking et al., 2011; Yu, 2012; Abdalla et al., 2016; Lin et al., 2022). Several studies have been conducted to study the effect of Fe and S on the C cycling and how the microbial community is able to promote the Fe and S cycling in freshwater environments (Straub et al., 2001; Emerson and Weiss, 2004; Fortin and Langley, 2005; Weber et al., 2006; Pester et al., 2010; Anantharaman et al., 2018).

Fe is the fourth most abundant element on the earth crust, and it is found in the aqueous phase at concentration range from nmol L^{-1} to mmol L^{-1} and in the sediments at concentration ranging from μg g^{-1} soil to mg g^{-1} soil (Frey and Reed, 2012; Kappler et al., 2021). The cycle of this element in the freshwater environment and its influence on the biogeochemical processes of several key elements , such carbon, nitrogen and sulfur have been the focus of several studies (Lovley et al., 2004; Melton et al., 2012; Hansel et al., 2015; Kappler et al., 2021; Dong et al., 2023; Liu et al., 2024). In the environment Fe can be found in two main redox states, ferric ion, Fe(III), and ferrous ion, Fe(II). Ferric ions, Fe(III), is poorly soluble at neutral pH and are found mainly in crystalline forms such in poorly order (hydr)oxides minerals, (*e.g.,* ferrihydrite ($Fe(OH)_3$)), or in more structure minerals (*e.g.,* goethite (α-FeOOH) and hematite (α-Fe_2O_3)) (Colombo et al., 2014). Ferrous ions, Fe(II), on the other hand, are more soluble at neutral pH, but can nonetheless be found in minerals such pyrite (FeS_2), siderite ($FeCO_3$) or vivianite ($Fe_3(PO_4)_2$) (Colombo et al., 2014; Herndon et al., 2017). In environments rich in organic carbon, petlands in particular, Fe is associated with the dissolved organic matter (DOM). This association influences not only the storage and mineralization of the organic C, but also the stability of the Fe (Li et al., 2023). In particular, Fe-DOM flocs and aggregates are able to increase the solubility of Fe(III) at circumneutral pH, and at the same time preserve Fe(II) from oxidation under oxic condition, which would be otherwise fastly oxidized to Fe(III) (Rue and Bruland, 1995; Daugherty et al.,2017). Generally speaking, in the freshwater ecosystem the iron cycle is spatially separated into zones dominated by oxidative process, in the top oxic and photic layer, and

reductive process in the anoxic layer below the water table. Starting from the top oxic and photic layer, Fe(II) can be oxidised biologically to Fe(III) (Kappler et al., 2021). Genera such as *Gallionella* and *Leptothrix* (Betaproteobacteria) are able to use dissolved oxygen (O_2) to oxidase Fe(II) (Equation 1). Species such as purple sulfur bacteria (e.g., *Thiodictyon sp.*), green sulfur bacteria (e.g., *Chlorobium ferrooxidans* strain KoFox), and purple non-sulfur bacteria (e.g., *Rhodopseudomonas palustris* TIE-1) can oxidase Fe(II) phototrophically without oxygen, while fixing bicarbonate as carbon source (Equation 2) (Widdel et al., 1993; Heising et al., 1999; Jiao et al., 2005; Croal et al., 2007; Emerson et al., 2010). At the same time, Fe(II) can be abiotically oxidised by dissolved O_2 to Fe(III) or vice versa Fe(III) can be reduced to Fe(II) by the action of reactive oxygen species (ROS) and light (Sulzberger, 2015; Kappler et al., 2021).

$$4\ Fe^{2+} + O_2 + 10\ H_2O \rightarrow 4\ Fe(OH)_3 + 8\ H^+ \quad (1)$$

$$4\ Fe^{2+} + HCO_3^- + 10\ H_2O + UV_{light} \rightarrow 4\ Fe(OH)_3 + H_2CO + 7\ H^+ \quad (2)$$

As a result of the oxidation, nearly all formed Fe(III) precipitates in deeper layers as poorly crystalline minerals (Kappler and Newman, 2004; Kappler et al., 2021).

In deeper anoxic layers, poorly crystalline Fe(III) and other Fe(III) minerals are used as electron sink by Fe-reducing microorganisms, such *Geobacter* and *Shewanella* (Lovley and Phillips, 1988; Myers and Nealson 1990; Roden, 2006; Weber et al., 2006). Dissimilatory metabolisms that can be coupled with the Fe(III) reduction include: oxidation of dissolved hydrogen (H_2) (Equation 3), oxidation of organic carbon compounds, such fatty acids (*e.g.* lactate) and CH_4 (Equation 4 and 5), oxidation of ammonia (NH_4^+) to various form of nitrogen (N), such as nitrogen gas (N_2), nitrite (NO_2^-) and nitrate (NO_3^-) (Equation 6), and oxidation of elemental sulfur (S^0) to sulfate (SO_4^{2-}) (Equation 7) (Brock and Gustafson, 1976; Caccavo et al., 1992; Lovley et al., 1992; Sivan et al., 2011; Zhou et al., 2016; Huang and Jaffé, 2018).

$$H_2 + Fe^{3+} \rightarrow 2\ H^+ + 2\ Fe^{2+} \quad (3)$$

$$lactate + 4\ Fe^{3+} + 2\ H_2O \rightarrow acetate + HCO_3^- + 4\ Fe^{2+} + 5\ H^+ \quad (4)$$

$$CH_4 + 8\ Fe(OH)_3 + 16\ H^+ \rightarrow CO_2 + 8\ Fe^{2+} + 22\ H_2O \quad (5)$$

$$NH_4^+ + 6\ FeOOH + 10\ H^+ \rightarrow NO_2^- + 6\ Fe^{2+} + 10\ H_2O \quad (6)$$

$$S^0 + 6\ Fe^{3+} + 4\ H_2O \rightarrow SO_4^{2-} + 6\ Fe^{2+} + 8\ H^+ \quad (7)$$

Fe(II) can then either diffuse to the upper oxic layer, or undergo microbial oxidation coupled to the reduction of NO_3^- to N_2 or to NH_4^+ (Equation 8 and 9) in the anoxic layer (Straub et al., 1996; Bryce et al., 2018).

$$10\ Fe^{2+} + 2\ NO_3^- + 24\ H_2O \rightarrow 10\ Fe(OH)_3 + N_2 + 18\ H^+ \quad (8)$$

$$8\ Fe^{2+} + NO_3^- + 21\ H_2O \rightarrow 8\ Fe(OH)_3 + NH_4^+ + 14\ H^+ \quad (9)$$

In freshwater environments, those processes occur cyclically and simultaneously contribute to the biogeochemical cycling of iron (Figure 1) (Weber et al., 2006; Melton et al., 2012; Kappler et al., 2021).

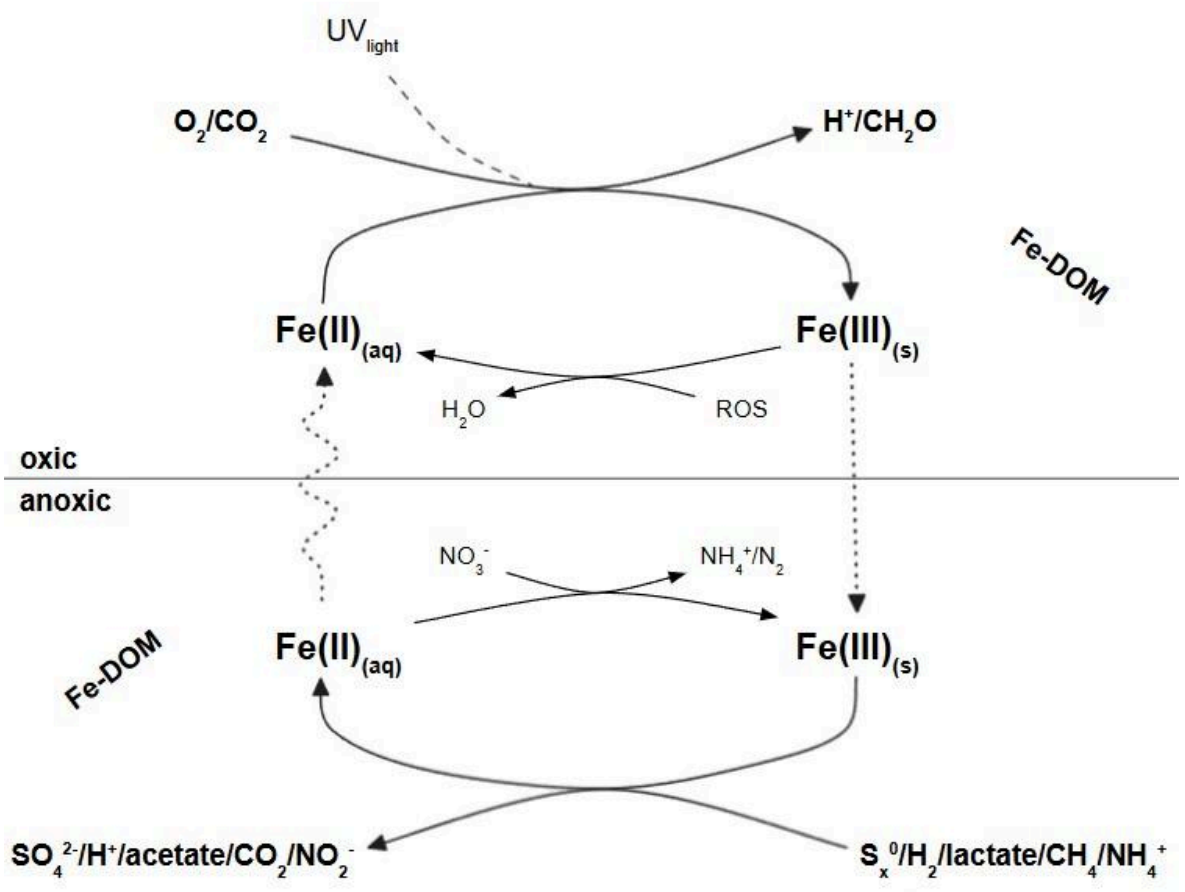

Figure 1. **Schematic overview of the Iron cycle in wetlands**. Abbreviation: Fe-DOM, Iron bound Dissolved Organic Matter.

S is the fifth most abundant element on earth and it plays a central role in maintaining the biological function of all organisms as it is used in the biosynthesis of amino acids, vitamins and enzymes. Sulfur biogeochemistry is relevant in many environments, where the redox transformation of sulfur can be coupled with the cycling of many other elements such as C, N and Fe (Wasmund et al., 2017; Wu et al., 2021; Zhou et al., 2024). Biogeochemical sulfur cycle is of particular interest, since large amounts of S have been released to the environment from coal burning and constant use of sulfur fertilizers (Rodhe, 1999; Hinckley et al., 2020). In the wetlands environments, S can be found in organic form, most notably dimethyl-sulfide (DMS), in inorganic forms dissolved in water, or in solid forms such as gypsum ($CaSO_4$) and pyrite (FeS_2)) (Canfield, 2004; Zhou et al., 2024). In the aqueous phase, sulfate (SO_4^{2-}) is ~ 28 mM in seawater, while its concentration is more variable in freshwater ecosystems, ranging between 0 to 6.6 mM (Holmer and Storkholm, 2001; Wasmund et al., 2017; Zak et al., 2021). The dissolved inorganic S, is found with redox states ranging from -2 (*e.g.*, HS^-) to the +6 (*e.g.*,SO_4^{2-}) (Wasmund et al., 2017; Zhou et al., 2025). In between, sulfur compounds have various valence states, such as 0 in the elemental sulfur/cyclic polysulfide (S^0_x), +2 in the thiosulfate ($S_2O_3^{2-}$), and +4 in the sulfide (SO_3^{2-}) (Wasmund et al., 2017; Zhou et al., 2024; Zhou et al., 2025). This broad range of redox states makes up a large part of the complexity of the sulfur cycle. In freshwater environments, SO_4^{2-} pool can undergo reduction to HS^- via two different pathways, including

(1) assimilative sulfate reduction, where bacteria and plant uptake S in order to synthesize organic sulfur compounds (*e.g.*, cysteine and DMS), and (2) dissimilatory sulfate reduction, where bacteria reduce sulfate for energy purpose (Lensmire et al., 2019; Wu et al., 2021; De Bont et al., 2022; Diao et al., 2023). Sulfur reducing bacteria (SRB), such those from genera *Desulfovibrio* and *Desulfomicrobium*, are ubiquitous in the anoxic layers and are able to use various electron donors for sulfate reduction. These include H_2 (Equation 10), and organic carbon compounds (*e.g.* acetate and propionate) (Equation 11 and 12) (Liamleam and Annachhatre, 2007; Muyzer and Stams, 2008; Wu et al., 2021; Zhao and Lu, 2023).

$$4\ H_2 + SO_4^{2-} + H^+ \rightarrow HS^- + 4\ H_2O \quad (10)$$

$$\text{acetate} + SO_4^{2-} \rightarrow 2\ HCO_3 + HS^- \quad (11)$$

$$\text{propionate} + 0.75\ SO_4^{2-} \rightarrow \text{acetate} + HCO_3 + HS^- + H^+ \quad (12)$$

Nearly formed HS^- can be then oxidized by sulfur oxidizer bacteria (SOB), first to S intermediates such S^0_x and $S_2O_3^{2-}$ and then to SO_4^{2-}, or directly to SO_4^{2-} (Lin et al., 2018). Two main communities are present in the freshwater oxic and photic layer, including phototrophs such as green sulfur bacteria (*e.g. Thiocapsa* and *Thiococcus*) and purple sulfur bacteria (*e.g. Chlorobium* and *Prosthecochloris*), and chemotrophs such as *Thiobacillus* and *Thiosphaera* (Lin et al., 2018). Phototrophs are able to oxidize sulfur under anaerobic conditions, using light energy for carbon fixation (Equation 13 and 14) (Lin et al., 2018). While chemotrophs use various electron acceptor such dissolved oxygen (O_2) (Equation 15 and 16), NO^{3-} (Equation 17, 18 and 19) and metal, as Fe(III) (Equation 20 and 21) and Mn(IV), in order to oxidase the S compounds (Brock and Gustafson, 1976; Kwon et al., 2014; Lin et al., 2018; Wu et al., 2021).

$$H_2S + 2\ CO_2 + 2\ H_2O \xrightarrow{\text{Light}} SO_4^{2-} + 2\ CH_2O + H_2 \quad (13)$$

$$H_2S + CO_2 \xrightarrow{\text{Light}} S^0_x + CH_2O + H_2O \quad (14)$$

$$H_2S + 2\ O_2 + H_2O \rightarrow SO_4^{2-} + 2\ H^+ \quad (15)$$

$$H_2S + 0.5\ O_2 \rightarrow S^0_x + H_2O \quad (16)$$

$$H_2S + 1.6\ NO_3^- + 1.6\ H^+ \rightarrow SO_4^{2-} + 0.8\ N_2 + 0.8\ H_2O \quad (17)$$

$$H_2S + 0.4\ NO_3^- + 2.4\ H^+ \rightarrow S^0_x + 0.2\ N_2 + 1.2\ H_2O \quad (18)$$

$$H_2S + 0.25\ NO_3^- + 2.5\ H^+ \rightarrow S^0_x + 0.25\ NH^{4+} + 0.75\ H_2O \quad (19)$$

$$3\ HS^- + 2\ Fe(OH)_3 + 2\ H^+ \rightarrow S^0_x + 2\ Fe^{2+} + 3\ H_2O \quad (20)$$

$$S^0_x + 6\ Fe^{3+} + 4\ H_2O \rightarrow SO_4^{2-} + 6\ Fe^{2+} + 7\ H^+ \quad (21)$$

HS^- can also exit the S cycle by binding with Fe(II) and precipitating as iron monosulfide (FeS) and FeS_2 minerals (Wei et al., 2023).

From the incomplete HS^- oxidation, S intermediates (*e.g.*, elemental sulfur and thiosulfate) can undergo microbial disproportionation, where the same S compound is simultaneously oxidized and reduced into two products with different valents state (Slobodkin and

Slobodkina, 2019). This particular metabolisms have been demonstrated in over 30 bacterial species across three main phyla (Proteobacteria, Thermodesulfobacteria, and Firmicutes). Most of characterized S-disproportionating bacteria are autotrophs, whereas a few freshwater genera (e.g., *Desulfovibrio*, *Desulfurella* and *Desulfocapsa*) couple disproportionation metabolism with heterotrophic growth (Bak and Cypionka, 1987; Peduzzi et al., 2003; Florentino et al., 2016; Slobodkin and Slobodkina, 2019). Known S intermediates that can undergo disproportionation are $S_2O_3^{2-}$ (Equation 22) and, in presence of ferrihydrite as sulfide scavenger, S(0) (Equation 23) (Finster, 2008; Slobodkin and Slobodkina, 2019; Wu et al., 2021).

$$S_2O_3^{2-} + H_2O \rightarrow SO_4^{2-} + HS^- + H^+ \quad (22)$$

$$3\ S^0 + 2\ Fe(OH)_3 \rightarrow SO_4^{2-} + 2\ FeS + 2\ H^+ + 2\ H_2O \quad (23)$$

Furthermore, the S intermediates can also reduce back to HS^- (Wu et al., 2021), representing an additional pathway transforming S intermediates. Microorganisms capable of performing this reductive sulfur transformation are often found to use H_2 or organic carbon as electron donor (Figure 2) (Wu et al., 2021).

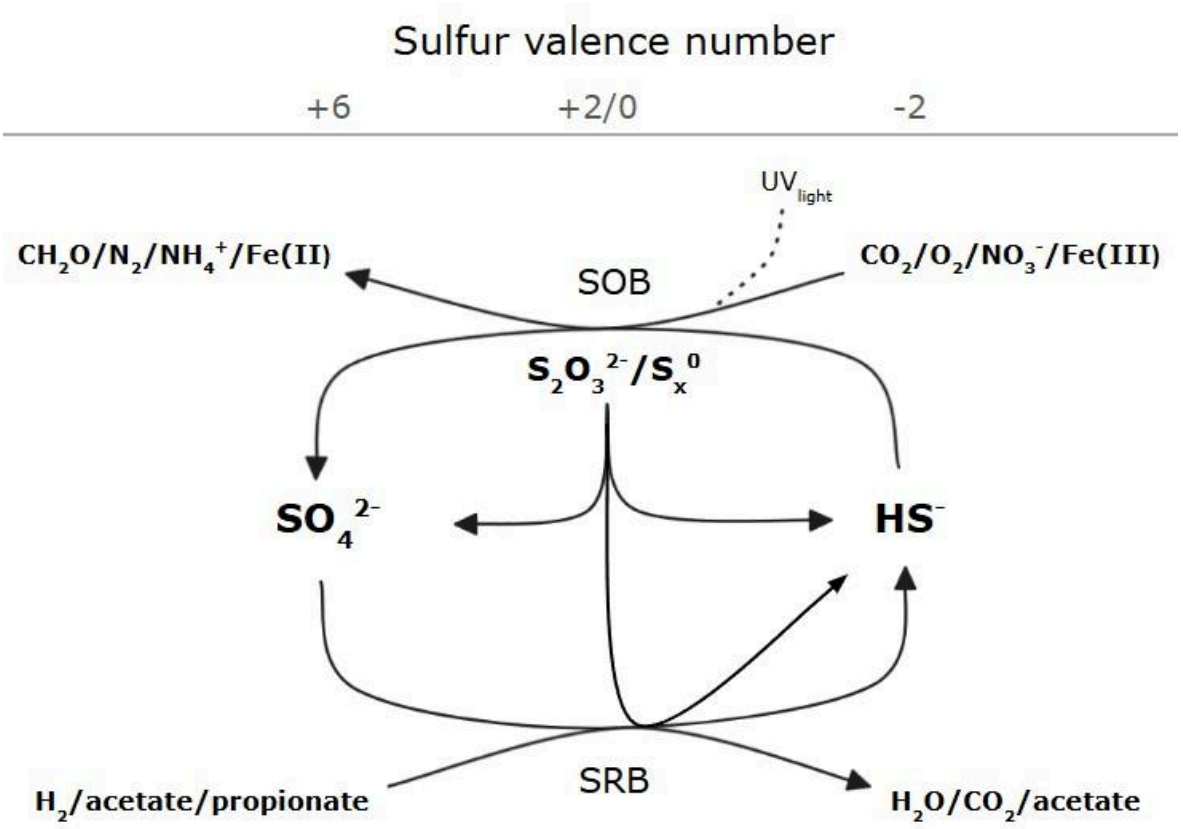

Figure 2. **Schematic overview of the sulfur cycle in wetlands**. Abbreviation: SOB, sulfur oxidising bacteria, SRB, sulfur reducing bacteria.

In peatland ecosystems, the fast turnover of the small sulfate pool (10-300 µM) makes studies of S intermediates of the primary importance. S intermediates such as thiosulfate can serve as a shunt in the S cycle, contributing to the rapid turnover of S (Jørgensen, 1990; Pester et al., 2010; Findlay and Kamyshny, 2017). In this sense, studies have been

conducted to investigate the microbials coupling of S and Fe cycles in the wetland (Kwon et al., 2014; Hansel et al., 2015). Nevertheless, studies on the $S_2O_3^{2-}$ oxidation in peatlands are missing. In this thesis, I investigated the coupling of $S_2O_3^{2-}$ oxidation to Fe(III) reduction and the microbial community involved in this reaction, focusing on its presence in peatland environments. To achieve this objective, I combined physiological experiments with molecular analyses on a peatland enrichment culture. My findings highlight select community members interconnected in a complex food web linking the cycle of the main elements such sulfur, iron, carbon and nitrogen.

Material and methods

Sediment samples, enrichment and cultivation

Enrichment culture from soil samples of Schlöppnerbrunnen II (Germany, 50°07'55''N, 11°52'52''E) was started by Dr. Song-Can Chen in order to probe iron-dependent thiosulfate oxidation in peatland soil by providing thiosulfate and ferrihydrite as the only electron donor and acceptor, respectively.

Schlöppnerbrunnen II consisting of a minerotrophic fen, slightly acidic (pH 4.8 - 5.5) characterised by an iron rich groundwater (Hädrich et al., 2019). This fen is particularly well studied, with several studies made over the years. In particular this fen has been constantly monitored-long time by the Limnological Research Station and Department of Hydrology of the University of Bayreuth. Data report from a long-term monitoring of the fen report, in the pore water, a concentration of total iron(II) of 0.1 to 6.1 mg L^{-1}, between the years 1987 to 2001 (N = 858), a concentration of sulfate of 0 to 22.1 mg L^{-1}, between the years 1987 and 2009 (N = 945) and always between the later a concentration of DOC (dissolved organic matter) of 6.4 to 150.3 mg L^{-1} (N = 919), and nitrate of 0 to 22 mg L^{-1} (N = 943) (Knorr, 2013). Rate of formation/consumption for iron(II), sulfate and CO_2, was also tested in the laboratory via microcosm incubation of fen soils. Formation/consumption rate for soils sampled at a depth of 10-20 cm was 430 nmol g (wet wt soil)$^{-1}$ d^{-1} for iron(II), -0.34 nmol g (wet wt soil)$^{-1}$ d^{-1} for sulfate, and 253 nmol g (wet wt soil)$^{-1}$ d^{-1} for CO_2 (N = 3) (Küsel et al., 2008).

Enrichment culture was cultivated in freshwater medium without sulfate (pH = 4.25) with following components: NH_4Cl 0.3 g/l, KH_2PO4 0.5 g/l, NaCl 1.0 g/l, $MgCl_2$ $6H_2O$ 0.33 g/l, and $CaCl_2$ $2H_2O$ 0.1 g/l. The basal medium was first autoclaved at 121 °C for 15 minutes and cooled down under anoxic atmosphere of 100% N_2, then, before use, 1 mL/L of each the following vitamins and trace elements was added: trace element solution, selenium-tungstate, riboflavin vitamin solution, B12 vitamin solution, 7 vitamine solution, thiamine.

Transfer of the enrichment culture was performed under constant flow of N_2:CO_2 80:20 in a 60 mL serum bottle provided with 0.3 g of synthetic ferrihydrite (see reagent preparation below), 5 mL of inoculum and 25 mL of freshwater medium without sulfate as previously described. The culture was then sealed with butyl-rubber stoppers, flush for a minute with N_2:CO_2. The culture was amended weekly with 200-500 µM of thiosulfate as electron donors. The culture was kept incubated without shaking in the dark for 28-35 days at 14 °C before the further transfer. Measurement of Fe(II) was performed routinely every 7-10 days. 16S rRNA gene sequencing was also performed on a select number of bottles during the enrichments.

Experimental designs

Chemical stability of thiosulfate in uninoculated freshwater media was tested under our experimental conditions. Duplicate 60 mL serum bottle was setted up, using 30 mL of freshwater medium without sulfate, added with vitamins and trace elements. A duplicate was provided with 0.3 g of synthetic ferrihydrite, while the other was kept as control without any

synthetic ferrihydrite. All bottles were prepared under constant flushing of N_2:CO_2 80:20. After closing the bottle with butyl-rubber stoppers, each bottle was flush for a minute under N_2:CO_2 80:20 and spiked with 5 mM of anoxic thiosulfate. Incubation was performed without shaking in the dark for 17 days at 14 °C. The bottle was sampled at 0, 1, 2, 3, 6, 8, 10, 14, 17 days in order to quantify the concentration of thiosulfate and sulfate using capillary electrophoresis (CE).

Thiosulfate oxidation coupled with iron reduction was tested in the enrichment culture (Figure 3). All treatments were set up in triplicates in 60 mL serum bottles using 25 mL of freshwater medium without sulfate and 5 mL of inoculum from the sediment-free, stable enrichment culture. The treatments were prepared in an anaerobic tent with an atmosphere of N_2:H_2 95:5 and further flushed with N_2:CO_2 80:20 for a minute after being closed with butyl-rubber stoppers in order to remove any trace of H_2. The experiment comprises five treatments. The first treatment consists of three replicate bottles, added with 0.3 g of synthetic ferrihydrite and periodical addition of 200 µM thiosulfate every three days. The second treatment consisted of the abiotic control, with the same condition of the test treatment but 5 mL of autoclaved (121 °C for 15 minutes) inoculum. The third treatment represented the thiosulfate-only control, without ferrihydrite and periodical addition of 200 µM thiosulfate every three days. The fourth treatment was the ferrihydrite-only with 0.3 g of ferrihydrite, here the same volume of thiosulfate added (0.6 mL) was substituted with an equal volume of anoxic water added every three days. Last treatment was culture-only control, where neither ferrihydrite nor thiosulfate was added, but a supplement of anoxic water was performed every three days. All treatments were incubated without shaking in the dark for 30 days at 14 °C. Cultures were sub-sampled at 0, 3, 6, 9, 12, 15, 18, 21, 24, 27 and 30 days after each spike of thiosulfate for quantification of the total Fe(II), the total sulfide, dissolved inorganic ions *(e.g.,* thiosulfate, sulfate). The culture was also sampled for molecular biology analysis at 0, 9, 21 and 30 days, after the precedently described sampling. At the end of the incubation the culture was further sampled for fluorescence microscopy.

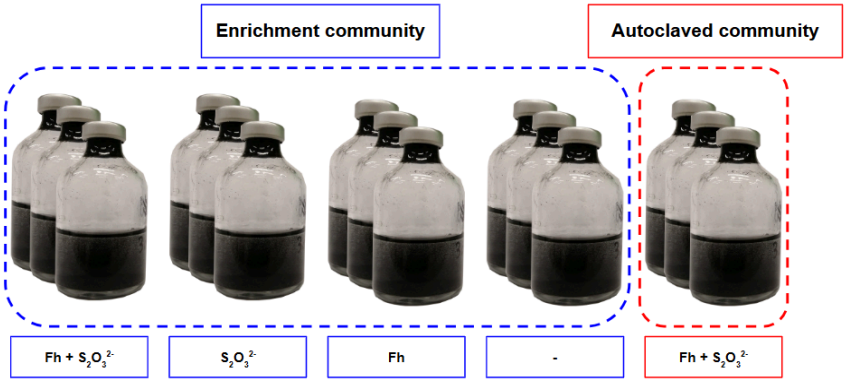

Incubation time (days)	0	3	6	9	12	15	18	21	24	27	30
Sampling	D + A	A	A	D + A	A	A	A	D + A	A	A	D + A + M

Figure 3. Thiosulfate oxidation coupled with iron reduction experimental design.

D = DNA extraction; A = Analytic measurement ($S_2O_3^{2-}$, SO_4^{2-}, HS^-, Fe(II)); M = Microscopy

Molecular biology analysis was conducted on the enrichment culture. The community composition at different growth stages of the enrichment was analyzed by 16S rRNA gene amplicon sequencing (see below). Community composition of the thiosulfate oxidation coupled-iron reduction experiment was also profiled similarly.

Analytic measurement

Total iron(II) was measured by the ferrozine assay (Wayne, 1988) as follows: 100 µL of a well mixed sample was sampled using a needle flush with 100% N_2 and fixed with 200 µL of 0.75 M HCl. The fixed sample was centrifuged at 12 044x g for 10 minutes and the supernatant transferred in a new tube. The well mixed supernatant was then diluted in a 96 well-plate to 100 µL final volume using 1 M HCl and stained for 5 minute in the dark with 100 µL of ferrozine reagent (0,1% w/v ferrozine in 50% w/v ammonium acetate). The sample was then measured at a wavelength of 562 nm using a M200Pro plate reader (Tecan, CH) and the concentration inferred by the interpolation with the calibration curve.

Total iron(II) calibration: Calibration for the measurement of the concentration of the total iron in the samples was done using Fe(II) standards with concentration, 0, 200, 400, 600, 800, 1000 µM. Briefly, a stock solution of 5 mM of $FeCl_2$ (Sigma-Aldrich, USA) was prepared in 1 M HCl, and diluted to the desired concentration with 1 M HCl. 20 µL, of each standard was then plated with 80 µL of 1 M HCl in a 96-wells plate. To each well 100 µL of ferrozine reagent was added in the dark. The plate was then incubated for 5 minutes in the dark before being measured at 562 nm with an M200Pro plate reader (Tecan, CH).

Total sulfide was quantified using the methylene-blue methods (Cline, 1969). Briefly, 100 µL of a well mixed sample was sampled using a needle flushed with 100% N_2. The sample was then fixed using 250 µL of 3% w/v zinc acetate and diluted with 900 µL MQ water. 100 µL of Clide´s reagent (20 g/L dimethyl-4-phenylenediamine and 45 g/L $FeCl_3$ in 25% v/v HCl) was well mixed to the fixed sample and incubated in the dark for 20 minutes. 200 µL of the stained solution was then plated in a 96-well plate and measured at a wavelength of 670 nm using an M200Pro plate reader (Tecan, CH) after a 5 seconds shaking in the machine. The concentration was calculated by interpolation of the data with the calibration curve.

Total sulfide calibration: Calibration for the measurement of the concentration of the total sulfide in the samples was done using Na_2S standards. Briefly, an anaerobic stock solution of 5 mM of Na_2S was prepared. For each standard duplicate was prepared as follows. 250 µL 3% w/v zinc acetate was used to fix 0, 1, 2, 5, 10, 20 µL of the basal solution and diluted with 1000 µL of MQ water, minus the relative amount of basic solution (100 µL used to dilute the stock solution to the desired concentration + 900 µL as protocol for the measurement) in order to obtain 0, 50, 100, 250, 500, 1000 µM standard. To each 100 µL of Cline´s reagent was added in the dark and after 20 minutes of incubation, 200 µL of solution was plated in a 96-well plate and measured at 670 nm with an M200Pro plate reader (Tecan, CH) after a 5 seconds shaking in the machine.

Capillary electrophoresis (CE) was used as follows in order to determine the concentration of thiosulfate, sulfate, organic acid, nitrite, and nitrate. 100 µL of well mixed culture was sampled using a needle flushed with 100% N_2 and diluted with 400 µL MQ water. The sample was then resuspended with a syringe inside the tube and filtered through a 0.2 µm pore membrane in a new tube. The filtrate was then stored at -20 °C until the measurement.

In order to be measured, the bare fused silica capillary (inner diameter: 75 µm, length: 72 cm) of a 7000D CE machine (Agilent Technologies, USA) was preconditioned twice every time the machine was switched on and once every time before a measurement. Two different methods were used in order to measure the sample (see below). In both cases the data was acquired from a diode array indirect UV-vis detector (DAD) at a wavelength of 350 nm with a bandwidth of 20 nm and reference at a wavelength of 205 nm with a bandwidth of 10 nm.

For the measurement of the inorganic ions (e.g., thiosulfate, sulfate, nitrite and nitrate), PMA buffer (2.25 mM pyromellitic acid, 0.75 mM hexamethonium hydroxide, 1.6 mM triethanolamine, and 6.5 mM NaOH pH 7.8 ± 0.1) was used as separation buffer. The sample was transferred in a CE plastic vial ((Agilent Technologies, USA) and mixed 1:1 with 50 µL of 1 mM $NaClO_3$ as internal standard. Each sample was injected for 3 s in the capillary (at 50 mbar) and measured at a voltage of - 30 kV (100 µA, 6 W) for a run time of 20 minutes. In the end, the area of the peaks data was normalized with the area of the peaks of both internal standard (ClO_3^-) and the peaks of Cl^- present in the medium. The concentration was then inferred from the normalised data using the calibration curve.

The organic acids were separated using the organic acid buffer for CE (Agilent Technologies, USA; pH = 5.6). After being melted, 100 µL of sample, from the -20 °C storage, was transferred in a CE plastic vial (Agilent Technologies, USA). Each sample was injected for 5 s in the capillary (at 50 mbar) and separated at a voltage of - 25 kV (100 µA, 6 W) for 20 minutes. The height of the peaks was then normalised with the height of the Cl^- peaks in the medium and the concentration inferred from the normalised data using the interpolation with the calibration curve.

Thiosulfate and Sulfate calibration: In order to measure the concentrations of thiosulfate and sulfate in the samples, a calibration with double standards $S_2O_3^{2-}/SO_4^{2-}$ was prepared. The double standard solution consists of 10 mM thiosulfate and 100 mM sulfate. The stocks were then diluted in a tube with freshwater media added with vitamins and trace elements in order to obtain the following standards, 0) 0 mM $S_2O_3^{2-}$/ 0 mM SO_4^{2-}, 1) 0.5 mM $S_2O_3^{2-}$/ 1 mM SO_4^{2-}, 2) 1 mM $S_2O_3^{2-}$/ 2 mM SO_4^{2-}, 3) 1.5 mM $S_2O_3^{2-}$/ 3 mM SO_4^{2-}, 4) 2 mM $S_2O_3^{2-}$/ 4 mM SO_4^{2-}, 5) 2.5 mM $S_2O_3^{2-}$/ 5 mM SO_4^{2-}. An aliquot of the stock was then diluted 5 times with MQ water and filtered through a 0.2 µm pore membrane and stored at -20 °C until the measurement. Measurement was done using the *inorganic ions* methods (precedently described) with each timepoint sample measurement.

Nitrite and Nitrate calibration: Standards preparation for the quantification of nitrate and nitrite concentration in the sample was done using double standards NO_2^-/NO_3^-. Briefly, the stock solution of 100 mM of NO_2^- and 100 mM of NO_3^- was prepared in MQ water, and then diluted to a final concentration of 25 mM using MQ water. The solution was then well mixed with freshwater media to the desired final concentration. Standards were prepared at 2 mM, 1 mM, 0.5 mM, 0.25 mM, 0.125 mM, and 0 mM. An aliquot of the stock solution was then diluted 5 times with MQ water and filtered through a 0.2 µm pore membrane and stored at -20 °C until the measurement. Measurement was done using the *inorganic ions* methods (precedently described).

Organic Acids calibration: The calibration curve was prepared starting from a 50 mM stock solution of short chain fatty acids (SCFA) comprising Formate, Acetate, D-Lactate,

Propionate, Butyrate and Succinate. Standards were prepared at a concentration of 2 mM, 1.5 mM, 1 mM, 0.5 mM, 0.25 mM, and 0 mM as follows. The stock solution was diluted to the desired concentration using freshwater medium. The various standards were then diluted 5 times with MQ water and stored at -20 ºC until the measurement. Measurement was done using the *organic acids* methods (precedently described).

Gas chromatography was performed on a gas sample per treatment (N = 1) (bottle #3, #6, #9, #12, and #15) taken from the thiosulfate oxidation coupled with an iron reduction experiment, approximately after 55 days by the end of the incubation. The sample was measured via gas chromatography (model TGA-6442-W-4T-PT-2He Valco Instruments Company Inc., USA). Briefly, the headspace of the bottle was mixed once with a sterile needle and a gas tight syringe. 2 mL of gas was then sampled for the analysis. Gas sample was then run in the gas chromatograph machine in He gas carrier for a total of nine minutes and the concentration of gas detected by a pulsed discharge helium ionization detector. Concentration of CO_2, CO, H_2 and CH_4, was determined automatically by the machine using the manufacturer's internal calibration.

Fluorescence microscopy

In order to perform microscopy, 1 mL of well mixed culture was sampled using a needle flushed with pure N_2. To fix the cells, 900 µL of the sampled culture were mixed with 100 µL of polyformaldehyde (PFA) to reach a final PFA concentration of 2%. The sample was then stored at 4 ºC for at least two days before subsequent analysis. The fixed samples were then treated with 500 µL of sodium-dithionite buffer (50 g/L $Na_2S_2O_4$ in 0,35 M Acetic Acid and 0,2 M sodium citrate Thamdrup et al., 1993) for 5 minutes at room temperature. 100 µl of the treated sample was then well mixed with 10 mL of MQ water, and immediately filtered on a black polycarbonate membrane filter with 0.2 µm pore. The cells on the membrane were then stained with 5 µL of DAPI in CitiFour (2 mg/mL) in the dark for 15 minutes at room temperature and visualized using a fluorescence microscopy. A single image was taken in order to visualize the culture.

Community analysis

DNA extraction was performed starting from 500 µL of well mixed culture using the DNeasy PowerSoil Pro Kits (Qiagen, Netherlands) following the manufacturer protocol and eluted in a final volume of 30 µL. The sample was then quantified by optical density at a wavelength of 260 nm using a Qubit 4 instrument (Thermo Fisher Scientific, USA) and stored at - 20 ºC. An aliquot of the stored sample was then send to the Joint Microbiome Facility (JMF) between the University of Vienna and the Medical University of Vienna in order to be sequenced for the 16S rRNA gene, V4 region, using the in house pipeline (Pjevac et al., 2021). Briefly, 2 uL of sample was amplify using 25 uL of DreamTaq Green PCR Master Mix (ThermoFisher; USA) and 0.25 µmol L^{-1} of 515F (5´-GTGYCAGCMGCCGCGGTAA-3´) forward primer (Parada et al., 2016) and 806R (5´-GGACTACNVGGGTWTCTAAT-3´) reverse primer (Apprill et al., 2015). PCR amplification was performed in a BIORAD T100 Thermal cycler (Bio-Rad, USA) with cycling condition as Table 1.

Initial denaturation	94 °C for 3 minutes	
Denaturation	94 °C for 45 seconds	30 cycles
Annealing	52 °C for 60 seconds	
Elongation	72 °C for 90 seconds	
Final elongation	72 °C for 10 minutes	

Table 1. PCR program optimized for 16S rRNA gene 515F and 806R primer amplification.

The PCR product was then purified and normalised to 25 ng with SequalPrep Normalization Plate Kit (Invitrogen, USA) following manufacturer instructions. 16 S PCR product were then multiplexing using Microsynth (Balgach, Switzerland) barcoding oligonucleotides performing a PCR reaction using 50 µl of DreamTaq PCR Master Mix (ThermoFisher, USA), 0.8 µmol L^{-1} barcode oligonucleotide and 10 µL of 16S PCR products. Amplification was performed as Table 2.

Initial denaturation	94 °C for 4 minutes	
Denaturation	94 °C for 30 seconds	7 cycles
Annealing	52 °C for 30 seconds	
Elongation	72 °C for 60 seconds	
Final elongation	72 °C for 7 minutes	

Table 2. PCR program optimized for barcoding primers amplification.

The amplicons were then pooled together and sequencing libraries were prepared using TruSeq Nano DNA Library Prep Kit (Illumina, USA) and indexed with TruSeq DNA Single Indexes Set A or B (Illumina, USA). Sequencing was performed using Illumina MiSeq 2 x 300 cycles pair-ends mode with prior preparation of the pooled sample using MiSeq Reagent kit v3 (Illumina, USA). Individual amplicon were extracted for the raw data using FASTQ workflow in BaseSpace (Illumina, USA) with default parameters PhiX contamination was filtered out using BBDuk (BBTools, Bushnell B), and demultiplexing was performed using the demultiplex python package (Laros JFJ). In the end, ASVs (amplicon sequence variants) were extrapolated using DADA2 R package version 1.14.1 (Callahan et al., 2016a) run on R version 3.6.1 (R Core Team, 2013) applying the developer recommended settings (Callahan et al., 2016b).

All ASV´s sequence obtain from the JMF, with an relative abundance equal or above 2 % in the sample, were then analysed using the BLAST tool of NCBI using with the default settings excluding unculture and environmental sequences from the default dataset, in order to identify the closest cultured relative and infer the ASV genera.

Reagents preparations

Synthetic ferrihydrite (Fh) synthesis: 200 mL of 0.1 M $FeCl_3$ solution (Roth, Germany) was neutralized to a pH of 7.4 ± 1 with 1 M NaOH and distributed in 50 mL Falcon tubes. Each aliquot was centrifuged at 11000 rcf for 5 minutes at 4 ^oC to pellet the ferrihydrite oxides and the supernatant was discarded. The pellet was then washed six times with MQ water and froze dry overnight. The resulting powder was stored in the dark at -20 ^oC for a maximum of 30 days. Before every use the ferrihydrite was grinded in fine particles using stone mortars.

Results

Thiosulfate stability in freshwater media

To test the chemical stability of thiosulfate towards iron(III) oxides, we incubated thiosulfate (5 mM) with and without ferrihydrite in the freshwater media over a period of 17 days. The experiment was conducted in order to test for abiotic reaction involving thiosulfate degradation in our media (treatment without ferrihydrite), and for test thiosulfate stability in the presence of iron(III) oxides (treatments with ferrihydrite).

Over the incubation periods, the thiosulfate measurement ($S_2O_3^{2-}$) remains stable at an average of 4.109 mM ± 0.031 mM (n.s. (non significative) variation, p-value = 0.18, *t*-test) in the presence of ferrihydrite, and at an average of 4.492 mM ± 0.028 mM (n.s. variation, p-value = 0.12, *t*-test) in the absence of ferrihydrite. It is interesting to note the slight discrepancy (p-value = 5.07e-16, *t*-test) between treatment with and without ferrihydrite. This discrepancy (p-value = 5.43e-14, *t*-test) was shown also for the sulfate (SO_4^{2-}) measurement, where the concentration was stable at 0.361 mM ± 0.008 mM (n.s. variation, p-value = 0.23, *t*-test) in the treatment with ferrihydrite and at 0.286 mM ± 0.014 mM (n.s. variation, p-value = 0.48, *t*-test) in the treatment without. This effect could be induced by the bonding between Fe(II) with thiosulfate and sulfate that lower the detectable concentration of the anions in the sample. In this hypothesis the presence of Fe(II) would likely be caused by the abiotic degradation of Fe(III) in Fe(II) induced by the equilibration of the reaction (Figure 4 and 5).

These results indicate that any change in thiosulfate concentration in the thiosulfate oxidation coupled with iron(III) reduction experiment should be regarded as biological processes. While presence of sulfate in the treatments could be attributed to the dissociation of the $ZnSO_4$ present in the trace elements solution added to the freshwater media rather than to the degradation of the thiosulfate added to the system.

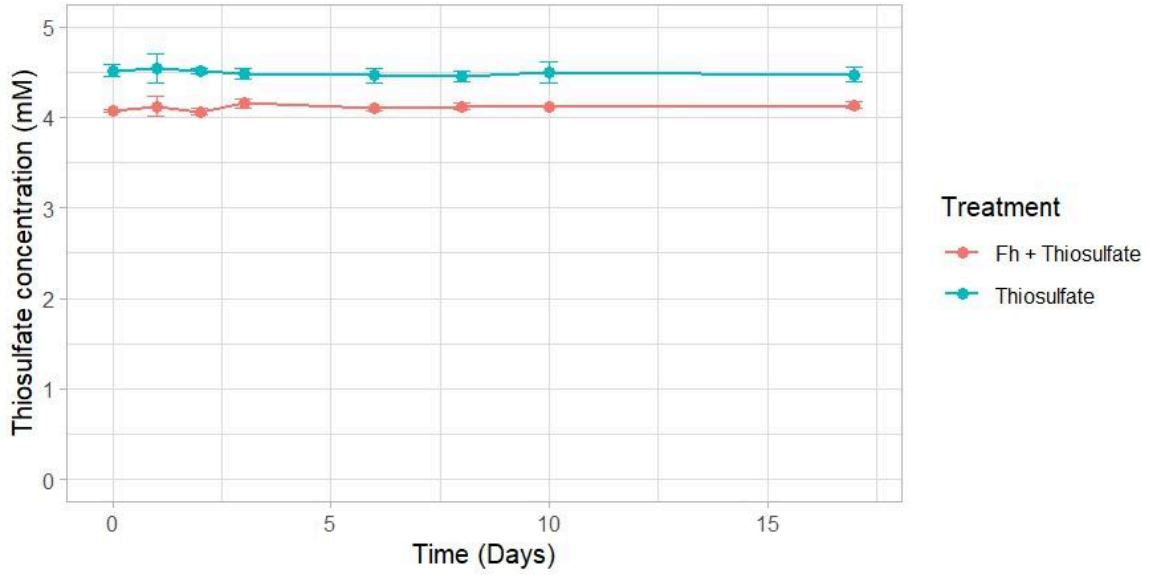

Figure 4. **Thiosulfate concentration over 20-day incubation in sterilized freshwater medium with and without ferrihydrite**.

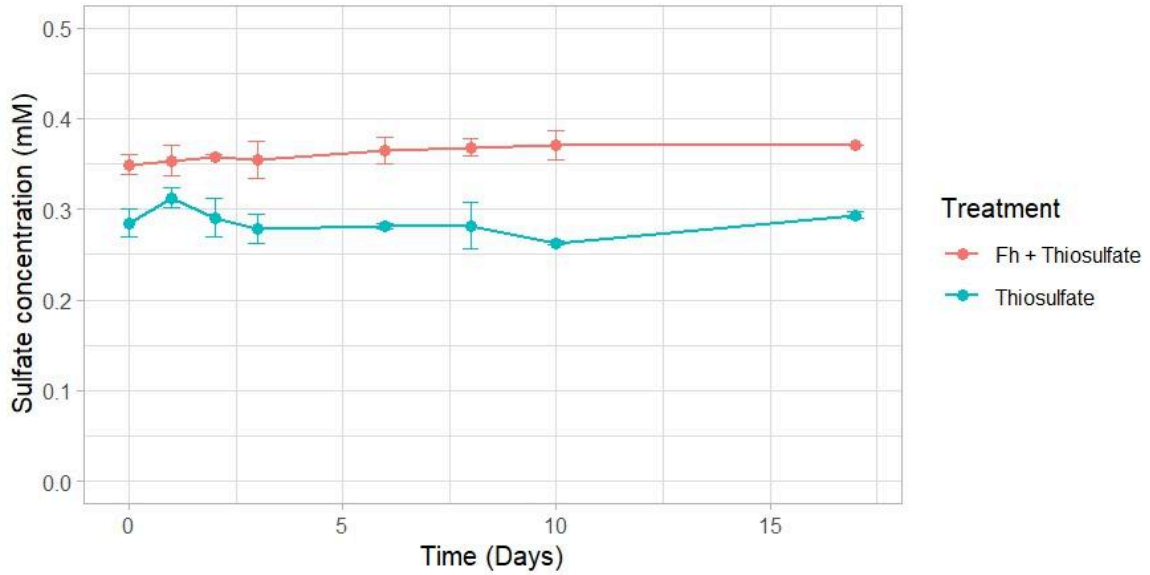

Figure 5. **Sulfate concentration over the abiotic incubation in freshwater media with and without ferrihydrite**.

Thiosulfate oxidation coupled with iron reduction

In order to test the coupling of thiosulfate oxidation and iron reduction in the enrichment culture, we set up five treatments in triplicate (N = 3) as seen in Figure 3. Treatment consists of enrichment culture incubated with either thiosulfate or ferrihydrite (Fe(III)) or combination of those. Abiotic treatments were also set up as reference in order to compare the abiotic behaviour of thiosulfate and ferrihydrite incubate together in the media. Treatments consist consequently as follows, in thiosulfate and ferrihydrite, only thiosulfate, only ferrihydrite, culture without any substrate and autoclaved control incubated with thiosulfate and ferrihydrite. Incubation was performed over 30 days with thiosulfate spike done in the relative treatments every 3 days. Measurement was also performed every 3 days. Incubation was monitored for thiosulfate consumption, sulfate and sulfide formation and iron(II) production. The results are listed below in the precedently mentioned order.

Thiosulfate ($S_2O_3^{2-}$) (Figure 6): Microcosms amended with thiosulfate show a stable concentration of 0.230 mM ± 0.028 mM (n.s. variation, ferrihydrite and thiosulfate treatment p-value = 0.72, thiosulfate-only treatment p-value = 0.08 *t*-test). No thiosulfate was detected in the microcosms amended with anoxic water. While the abiotic control (ferrihydrite + thiosulfate + autoclaved community), shows an average final increase of 1.621 mM ± 0.014 mM (p-value = 5.72e-5, *t*-test). An interesting point is notice that, as opposed as observed in the thiosulfate stability in freshwater media, the average starting concentration of thiosulfate in the treatment with ferrihydrite was not significantly lower (0.210 mM ± 0.019 mM) if compared with the average concentration in the treatment without (0.251 mM ± 0.019 mM) (n.s. variation, p-value = 0.32, *t*-test). Another interesting point can be observed if we take in consideration the average increase per addition of thiosulfate in the abiotic control, where the average increase was 0.147 mM ± 0.051 mM per addition, slightly lower to average concentration in the other ferrihydrite and thiosulfate biotic treatment (p-value = 7.83e-8, *t*-test).

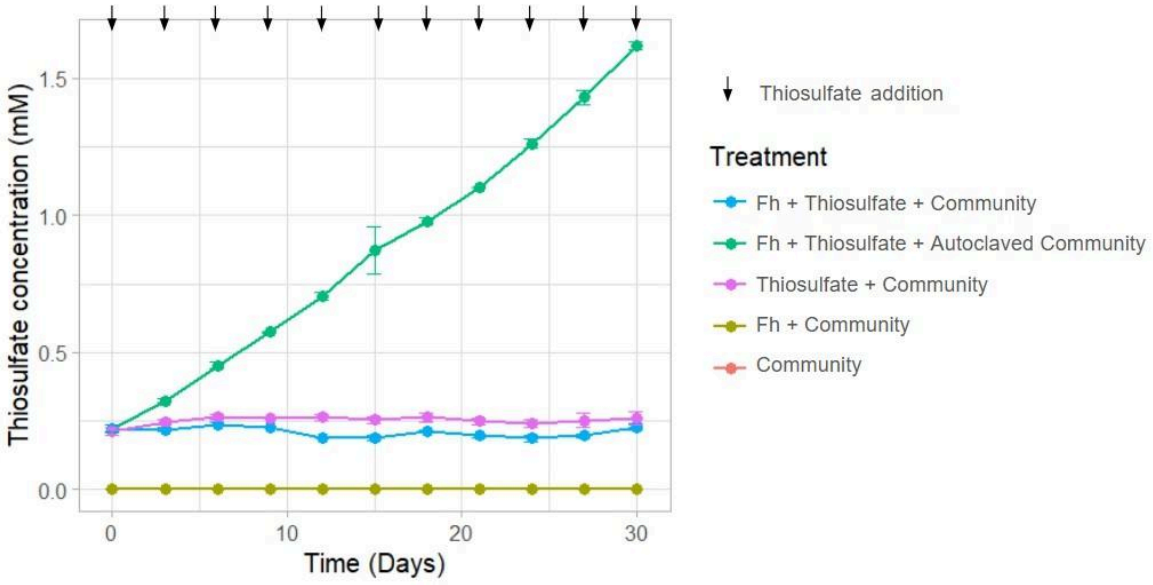

Figure 6. **Thiosulfate concentration (mM) over the incubation in the thiosulfate oxidation coupled with an iron reduction experiment**. It can be observed how, in the autoclaved control, the concentration rises steadily with each addition. While, in the active treatment amended with thiosulfate, the stable concentration is caused by the periodic additions performed before each measurement. No thiosulfate is detected in the treatments not amended with thiosulfate.

Sulfate (SO_4^{2-}) (Figure 7): Constant increase in the sulfate concentration was observed in the active treatments supplement with thiosulfate. The total amount of sulfate formed was 2.216 mM ± 0.034 mM (p-value = 7.86e-5, *t*-test) in the active culture incubated with thiosulfate and ferrihydrite. While in the treatment with thiosulfate only, the increase was 2.384 mM ± 0.039 mM (p-value = 9.02e-5, *t*-test). Sulfate concentrations were mostly stable, with only a slight increase in the other treatments. In the abiotic control (amended with thiosulfate) the increase was 0.181 mM ± 0.027 mM (p-value = 7.57e-3, *t*-test), while in the treatments amended with MQ water the increase was 0.095 mM ± 0.002 mM (p-value = 2.31e-4, *t*-test) in the culture only treatment, and 0.057 mM ± 0.003 mM (p-value = 9.86e-4, *t*-test) in the ferrihydrite only control. Congruous with the precedent observation, we observed that the sulfate concentration in the treatments with ferrihydrite is slightly differ from the treatments without ferrihydrite. At time 0 in fact, in the presence of ferrihydrite, the average measurement was lower (0.595 mM ± 0.019 mM) if compared with the measure taken in treatments without ferrihydrite (0.868 mM ± 0.023 mM) (p-value = 7.61e-12, *t*-test).

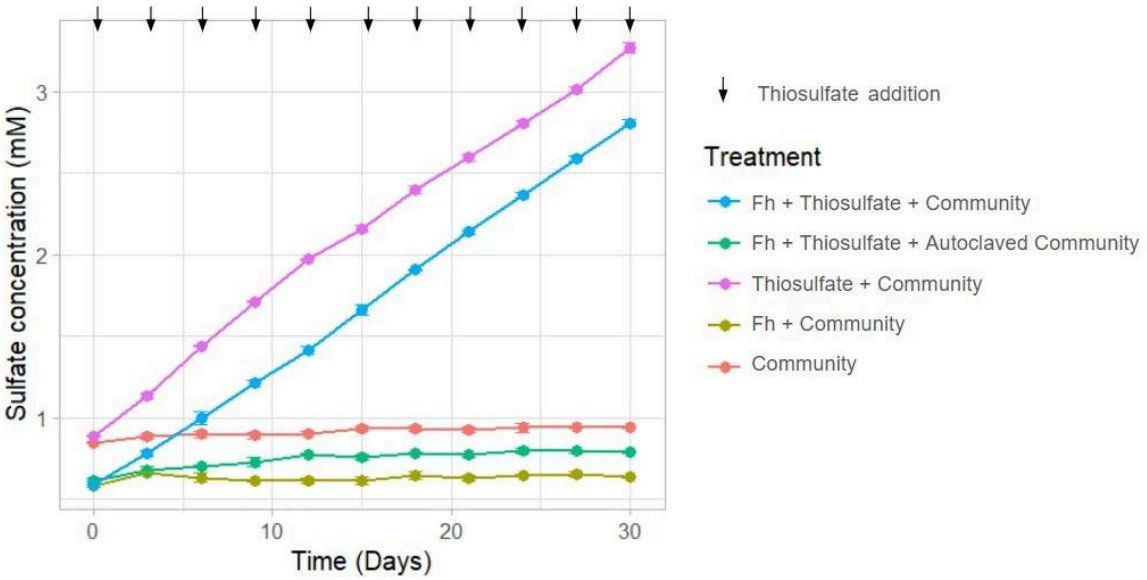

Figure 7. **Sulfate concentration (mM) over the incubation in the thiosulfate oxidation coupled with an iron reduction experiment**. The constant formation of sulfate can be observed in the active treatment amended with thiosulfate. No sulfate is generated in the other treatments.

Total sulfide (HS^-) (Figure 8): Similarly to the sulfate results, increase in the sulfide concentration in the active treatment amended with thiosulfate was observed. The total amount of sulfide formed was 0.372 mM ± 0.027 mM (p-value = 1.73e-3, *t*-test) in the treatment with ferrihydrite and 0.680 ± 0.140 mM (p-value = 1.39e-2, *t*-test) in the treatment without. No sulfide formation was observed in the other treatments, where the starting concentration of sulfide decreases to zero (abiotic treatment p-value = 5.65e-3, ferrihydrite-only treatment p-value = 1.55e-3, and community-only treatment p-value = 7.16e-3 *t*-test).

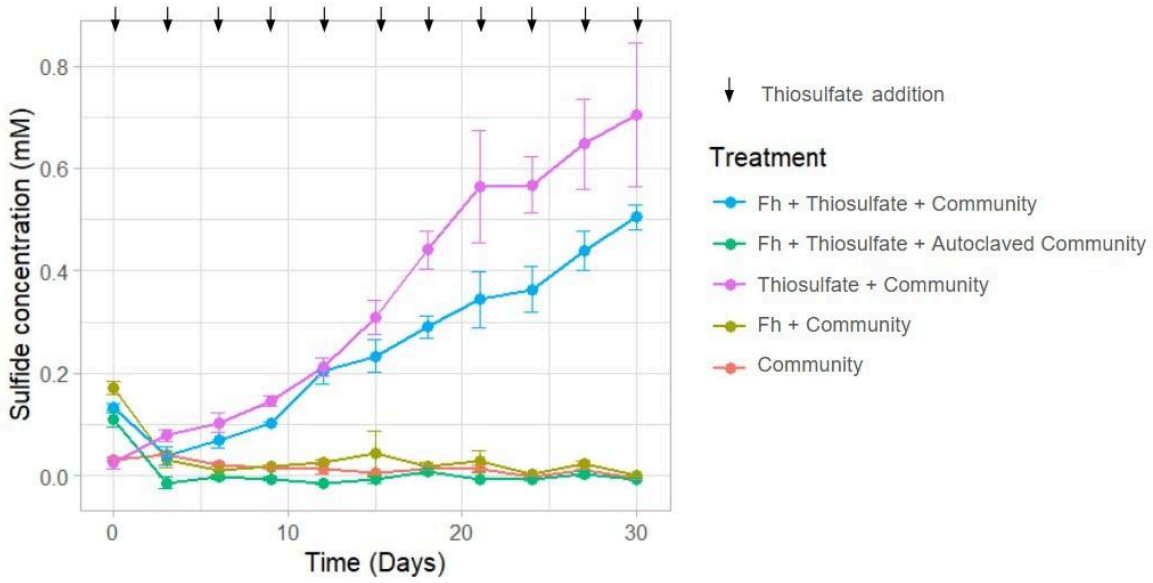

Figure 8. **Sulfide concentration (mM) over the incubation in the thiosulfate oxidation coupled with an iron reduction experiment**. It can be observed how, in the active treatments amended with thiosulfate, sulfide (~0.5 - 0.7 mM) are formed. Consumption of sulfide can be, viceversa, observed in the other treatments.

Total iron(II) (Fe^{2+}) (Figure 9): The massive iron(II) formation (6.753 mM ± 0.141 mM p-value = 1.45e-4, *t*-test) was observed in the active cultures incubated with ferrihydrite and thiosulfate amendment. Smaller increase in Fe(II) was also detected in the thiosulfate only and ferrihydrite only controls, where the increase was 1.280 mM ± 0.270 mM (p-value = 1.45e-2, *t*-test) and 1.285 mM ± 0.288 mM (p-value = 1.63e-2, *t*-test), respectively. No iron(II) increase was detected in the abiotic control (n.s. variation, p-value = 0.18, *t*-test) and in the community only control (n.s. variation, p-value = 0.13, *t*-test).

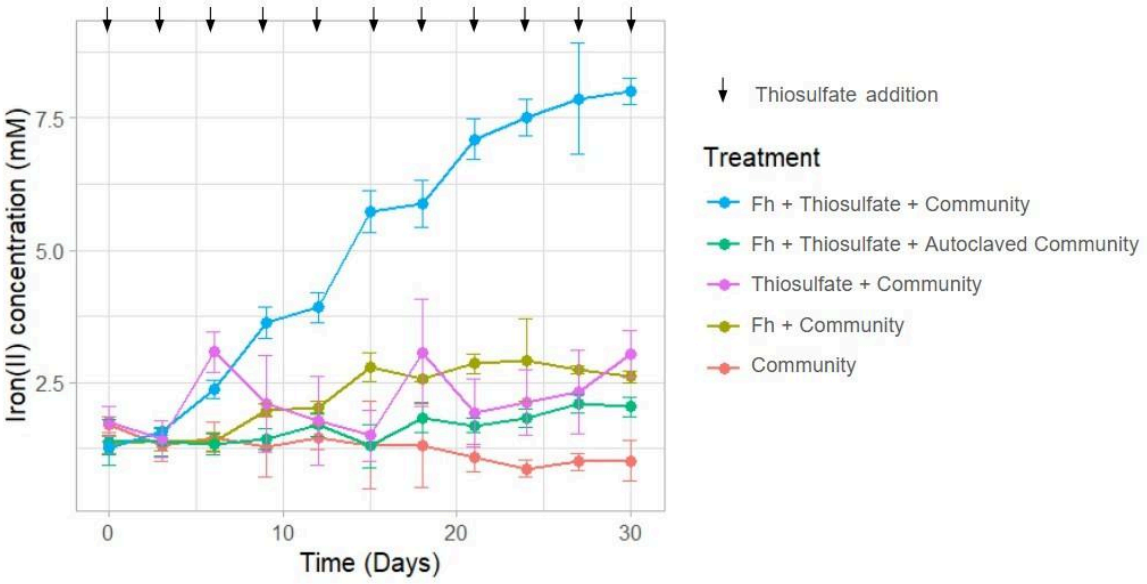

Figure 9. **Iron(II) concentration (mM) over the incubation in the thiosulfate oxidation coupled with an iron reduction experiment**. Formation of reduced iron can be observed only in the treatment incubated with thiosulfate and ferrihydrite.

Gas chromatography

Measurement of the headspace composition for one bottle per treatment (N = 1) (bottle #3 (Thiosulfate + ferrihydrite + culture), #6 (Thiosulfate + ferrihydrite + autoclaved culture), #9 (Thiosulfate + culture), #12 (Ferrihydrite + culture), and #15 (Culture only)) was performed after 55 days from the end of the incubation in order to assess the quantity of CO_2 present. The measure was performed as an indirect method in order to investigate the fixation of inorganic carbon by the culture. Must be noted here that we assume that the pH did not change between treatments since the change of pH would result in an equilibration between the CO_2 present in the headspace and the carbonate/bicarbonate buffer present in the media (Figure 10).

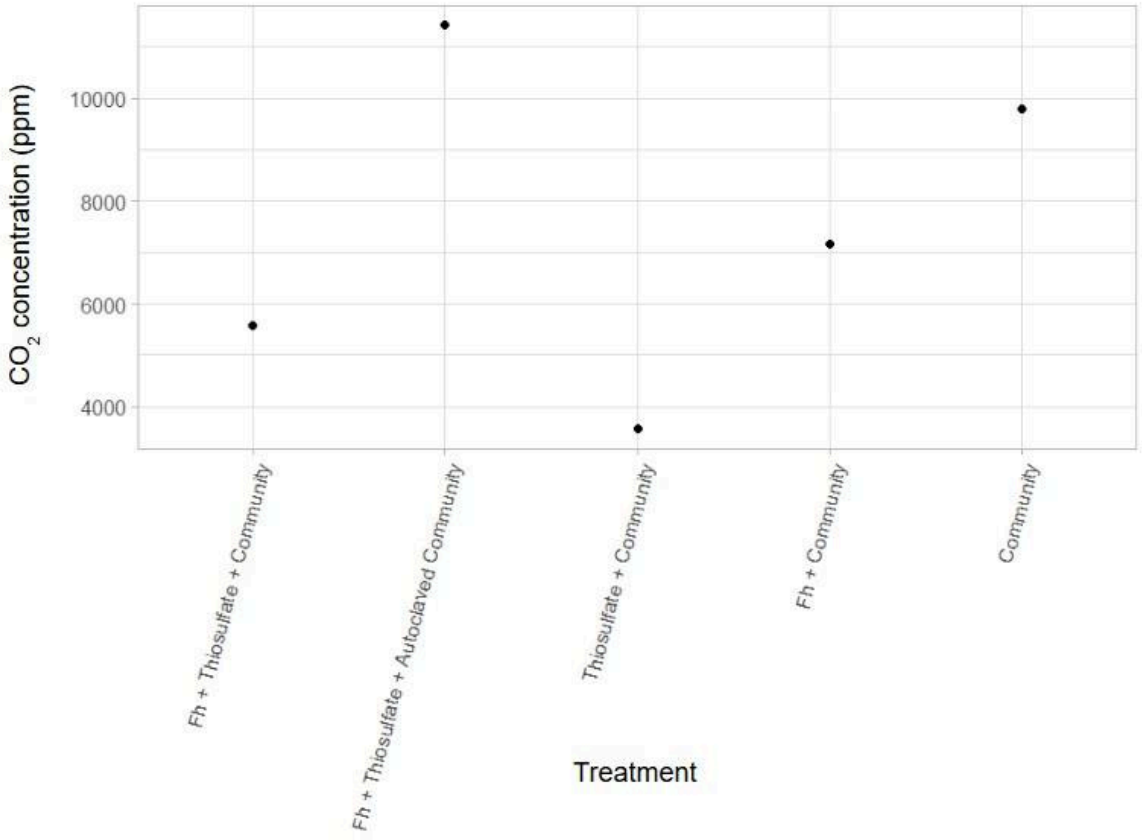

Figure 10. **Headspace CO_2 concentration (ppm) after the incubation of the thiosulfate oxidation coupled with an iron reduction experiment**. It can be observed that the highest concentration is shown by the abiotic control, while lower concentrations are present in the culture incubated with thiosulfate only or with thiosulfate and ferrihydrite.

Fluorescence microscopy

Fluorescence microscopy was employed to visualize the culture, enabling a qualitative assessment of cell density after 30 days of incubation and providing complementary data to integrate with DNA concentration measurements. Characterization was made by DAPI staining and shows differences in cell density in the culture incubate with thiosulfate and ferrihydrite. Smaller increase in cell density can be also observed in the control with either thiosulfate only or ferrihydrite only if compared to the culture only treatments (Figure 11).

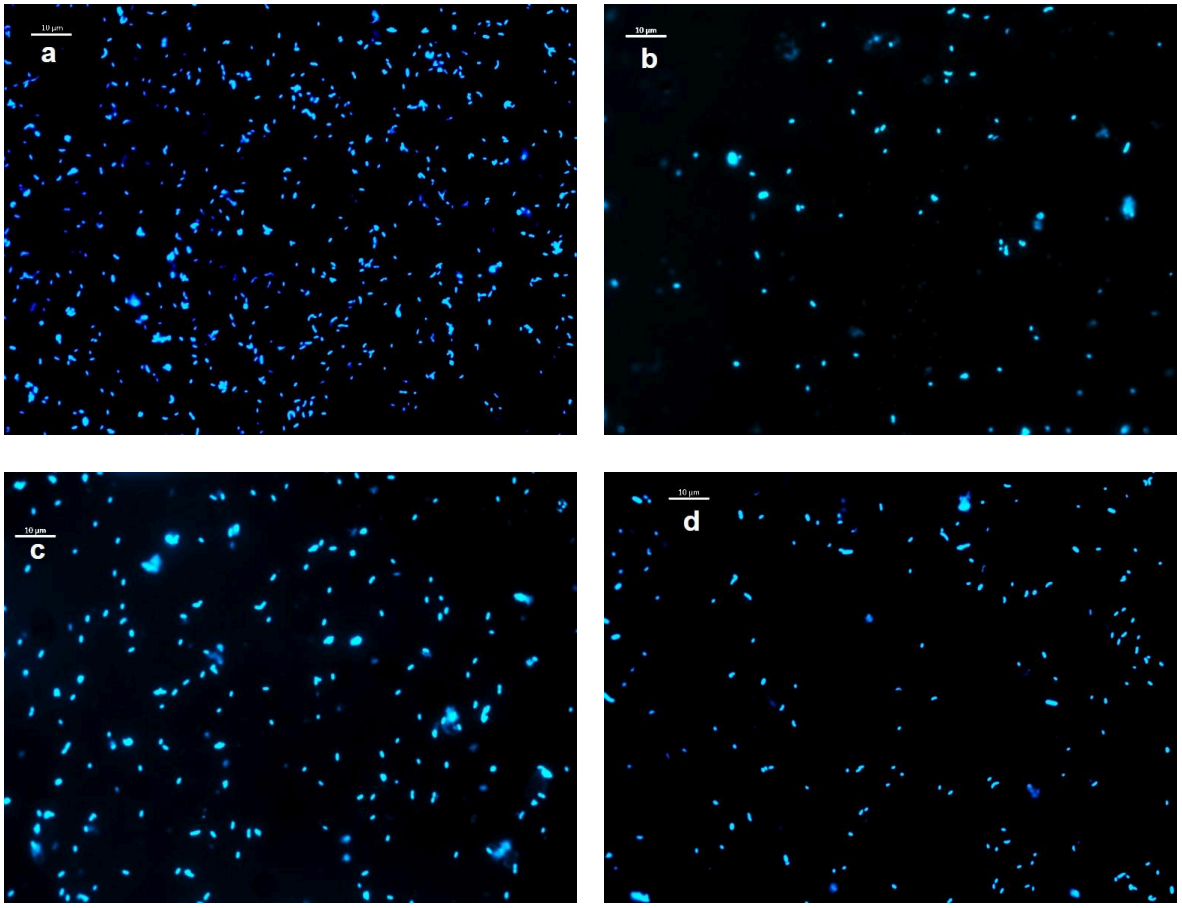

Figure 11. **Microscopic characterization (scale bar, 10 µm) of the enrichment culture from the thiosulfate oxidation coupled with an iron reduction experiment.** The cells are visualized by DAPI staining. Figure shows the culture density on **a**, ferrihydrite and thiosulfate; **b**, without any substrate; **c**, with thiosulfate only and **d**, with ferrihydrite only.

DNA extraction yields

DNA yields, from the DNA extraction, were used to integrate the fluorescence microscopy result in order to assess the growth of the culture provided with the various substrates from the thiosulfate oxidation coupled with an iron reduction experiment.

The observed increase in the amount of extracted DNA amounts to 2.51 ± 0.37 ng/µL (p-value = 7.26e-3, *t*-test) in the treatments incubated with thiosulfate and ferrihydrite. While in the other treatments the increase was not significant. With treatments incubate with only thiosulfate increasing of 0.16 ± 0.12 ng/µL (n.s. variation, p-value = 0.16, *t*-test), treatments incubated with only ferrihydrite increasing of 0.41 ± 0.25 ng/µL (n.s. variation, p-value = 0.10, *t*-test), while the control without any substrate provided (culture only) increases of 0.07 ± 0.04 ng/µL (n.s. variation, p-value = 0.12, *t*-test) (Figure 12). DNA extraction was also performed on two samples (N = 2) from the abiotic control after 30 days of incubation, but quantification was, as expected, too low to be detected with our methods.

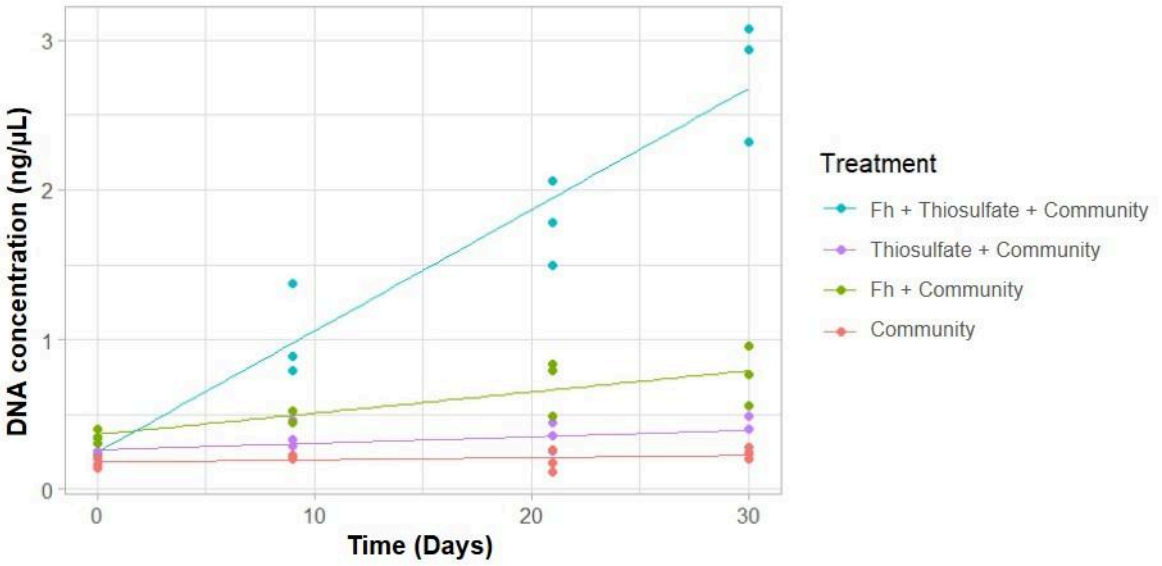

Figure 12. **DNA concentration (ng/µL) obtained from the nucleic acid extraction performed on the biotic treatments of the thiosulfate oxidation coupled with an iron reduction experiment**. The increase in DNA concentration can be observed in the culture incubated with both ferrihydrite and thiosulfate (blue dot). No significant growth is shown in the culture incubated with thiosulfate only (violet dot), ferrihydrite only (green dot), or without any substrate (orange dot).

Community profiling

Each microcosm (all treatments with the exception of the abiotic control) was profiled at day 0, 9, 12 and 30 via the V4 region of the 16S gene, in order to identify the component and evolution of the community incubated with the different substrate (Figure 13). Results show a depth of the sequencing of 10 069 ± 2 812 reads per sample across all time points.

At the time 0, the community composition was uniformly composed across treatments, consisting in *Thiovibrio* sp. and *Desulfosporosinus* sp.. After 9 days, a more diverse community emerged, it must be noted that *Thiovibrio* sp. and *Desulfosporosinus* sp. remain present in all treatment except in the thiosulfate-only where *Desulfosporosinus* sp. was not present above the 2 % relative abundance. The new members of the community comprises, in the treatment incubated with ferrihydrite, of *Geobacter* spp., *Trichlorobacter* sp., and *Desulfovibrio* sp. while, in the community-only, of *Pseudomonas* sp.. From day 9 to the day 30 of the incubation this genera remained mostly unchanged. An expectation was represented by *Geobacter* sp. in the culture-only treatment, detected from day 21, it was increased in abundance by the 30th day. Other exception are represented by *Mesoterricola* sp., detected in the treatment incubated with ferrihydrite and thiosulfate only at day 9 and in the treatment amended with thiosulfate-only at days 21 and 30, *Pseudomonas* sp. in the ferrihydrite-only treatment, detected only at day 9, and *Geotalea* sp., detected in the ferrihydrite-only treatment at day 30 only.

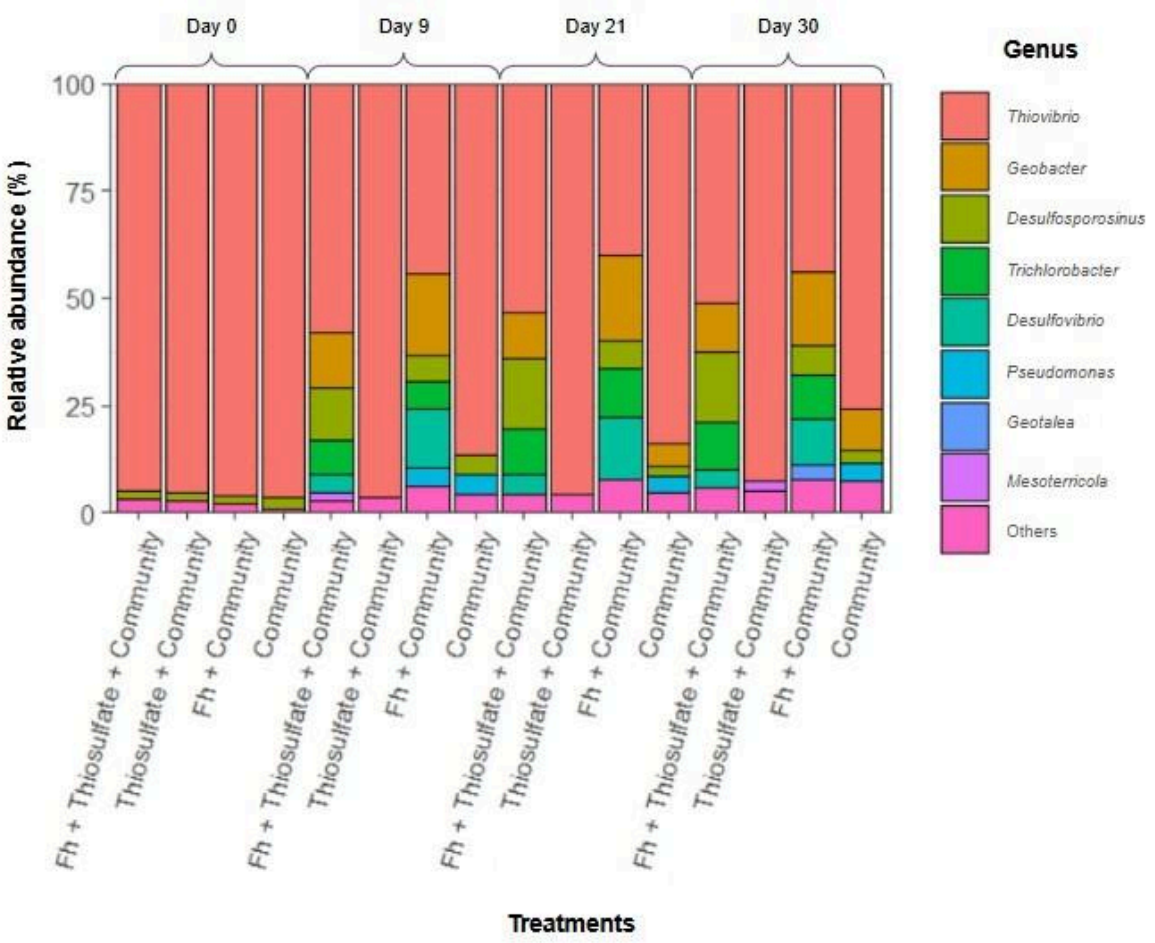

Figure 13. **Relative abundance (%) of the 16S rRNA gene, color coded base on the genus, from the profiling of the biotic treatments of the thiosulfate oxidation coupled with an iron reduction experiment**. We could see the complexity of the community in the presence of ferrihydrite while remaining mainly composed by *Thiovibrio* sp. in the treatment amended with thiosulfate-only or in the community only treatment.

Discussion

As we previously see, wetlands iron (Fe) and sulfur (S) cycle tightly link each other as well as with the cycle of some of the other major elements, such as nitrogen (N) and carbon (C). Although this close relationship and the importance that these two cycles have in the wetlands ecosystem, studies on the coupling of these two cycles are scarce. In particular the relation between thiosulfate oxidation and iron reduction, although observed (Thamdrup et al, 1993; Flynn et al., 2014; Berg et al., 2019), remains largely unexplored and cryptic to understand. Is unclear in fact how this reaction unfolds, if the process is directly coupled through microbial enzymatic activity or if it is indirectly mediated by intermediary electron carriers, such as soluble organic or inorganic electron shuttles.

In this thesis, starting in the thiosulfate oxidation coupled with iron reduction experiment, the stable concentration of thiosulfate in all the biotical treatments amended with thiosulfate indicates the complete consumption, between additions, of thiosulfate by the community. It is worth remembering that measurements were done after the addition, so the concentration measured corresponds to the quantity of thiosulfate added. By contrast, the concentration of thiosulfate in the abiotic treatment accumulates steadily over time, indicating that no biological process, or abiotic one, is in progress in the treatment. The biological consumption of thiosulfate is also correlated to the steady increase in the concentration of sulfate. Whereas, in the other treatments sulfate concentration remains unchanged. Overall, the comparable thiosulfate depletion, and sulfate formation, in both treatments amended with thiosulfate (with and without ferrihydrite) suggests that thiosulfate oxidation is likely independent from ferrihydrite reduction in the enrichment community.

Consumption of thiosulfate in the biotical treatment amended with thiosulfate was also associated with the formation of trace amounts of sulfide in the culture. While in no other treatments sulfide formation is observed. Based on the production of both sulfate and sulfide from the thiosulfate, a potential explanation is that the community was able to disproportionate the thiosulfate. This is further supported by the stable presence of *Thiovibrio sp.* as the main ASV in the incubation amended with thiosulfate only (95 % ± 1.9 %). The closest relative, *Thiovibrio frasassiensis* strain RS19-109^{T}, is in fact able to disproportionate thiosulfate under autotrophic growth conditions (Aronson et al., 2023). On the other hand, the observed fraction between the production of sulfate and sulfide differs significantly from the expected theoretical yields. Our expectation would consist in a fraction close to 1 (Equation 22), or even smaller as reported from the literature. However, the resulting fraction between the concentration of sulfate and the concentration of sulfide obtained in our experiment was 5.5, far from our expectation from the theoretical value (Jørgensen, 1990; Jackson and McInerney, 2000; Slobodkin and Slobodkina, 2019).

$$S_2O_3^{2-} + H_2O \rightarrow SO_4^{2-} + HS^- + H^+ \quad (22)$$

This could imply a considerable influx of electrons directed to the carbon fixation. Even considering that some of the sulfide can diffusion to the headspace in gaseous form or that some of the sulfur could be converted in elemental sulfur (S^0_x) by the abiotic reaction with ferrihydrite. But even in these later cases, the decrease in sulfide concentration recovered would have minimal effect on the fraction since most of the sulfur has been recovered in the

measurements. Namely 95% in the thiosulfate only treatments and 80% in the treatments incubate with thiosulfate and ferrihydrite.

Fixation of inorganic carbon could, in this case, lead to the formation of volatile fatty acids VFAs), such lactate or formate. Those compounds could be then used by other members of the community for their metabolisms.

In the treatment amended only with thiosulfate this would translate in *Thiovibrio sp.* able to couple disproportionation with fixation of inorganic carbon, which is abundantly present in the media both dissolved in bicarbonate/carbonate buffer and in the headspace as CO_2 gas. This appears to be supported by measurements of the headspace gas composition. Preliminary testing found a lower concentration of CO_2 in the treatment amended with thiosulfate compared to the treatment with ferrihydrite alone and the abiotic control. However, it must be noted that testing was performed on only one bottle, requiring additional measurements to confirm the trend. If this is the case, this would indicate that the carbonate was used in the media. Since the utilization of the carbonate in the media would modify the concentration of CO_2 in the headspace in order to maintain constant equilibrium between the dissolved carbonate and the gaseous CO_2. Here it must be noted that this outcome may be also caused by changes in the pH of the media, of which we have no data available.

More complicated would be in the treatments amended with thiosulfate and ferrihydrite, where ferrihydrite is reduced to Fe(II) likely via both abiotic and biotic reaction.

Abiotically, the sulfide (HS^-) produced could lead to the chemical reduction of the ferrihydrite, resulting in the formation of elemental sulfur (S^0_x) (Equation 24) (Dos Santos Afonso and Stumm, 1992; Thamdrup et al., 1993; Ionescu et al., 2015). This process, although likely present, could contribute only in minimal part to the total Fe(II) formed. We base this assumption on the total sulfur recovery, as most of it was recovered as sulfide and sulfate. Only a minimal portion, approximately 20%, could have potentially been transformed into elemental sulfur (S^0_x), possibly even less, considering that some of the unrecovered sulfur could have been sulfate adsorbed by iron oxides (as observed in the thiosulfate stability in freshwater media experiment) or escaped into the headspace as sulfide in gaseous form. Consequently, we can assume that most of the recovered Fe(II) was biotically reduced by the enrichment community, as elemental sulfur (S^0_x) could have contributed only partially to the reduction of ferrihydrite to Fe(II).

$$3\ H_2S + 2\ FeOOH \rightarrow S^0 + 2\ FeS + 4\ H_2O \qquad (24)$$

Biotically, as observed in the thiosulfate-only treatments, thiosulfate oxidation occurs independently of ferrihydrite presence in the system. This suggests that the coupling between thiosulfate oxidation and iron reduction, with ferrihydrite as the final electron acceptor, is indirect and mediated by an unknown intermediary electron carrier. This electron carrier could be then oxidized to facilitate ferrihydrite reduction. This possibility seams supported by the presence in the enrichment culture of *Geobacter* spp. and *Desulfovibrio* sp., genera well known for their ability to reduce iron minerals (Coleman et al., 1993; Li et al., 2006; Hori et al., 2015; Yang et al., 2021).

The most plausible electron carrier would be the volatile fatty acids (VFAs). Those would be derived from the fixation of the inorganic carbon mediated by *Thiovibrio* sp., as we proposed for the thiosulfate only treatments, and would be re-oxidised to CO_2 by the reduction of

ferrihydrite (Figure 14). This possibility is further strengthened by the known ability of *Geobacter spp.* to oxidase acetate into CO_2 by respiring ferrihydrite (Caccavo et al., 1994; Küsel et al., 2008). This possibility will be, also, coherent with the gas measurement from the headspace of the culture incubated with thiosulfate and ferrihydrite, where the CO_2 concentration found is higher if compared to the thiosulfate only control, but lower if compared to all the other treatments. Probably indicate that some of the CO_2 fixed in short fatty acids during the thiosulfate oxidation is reconverted back to CO_2 by the reduction of Fe(III).

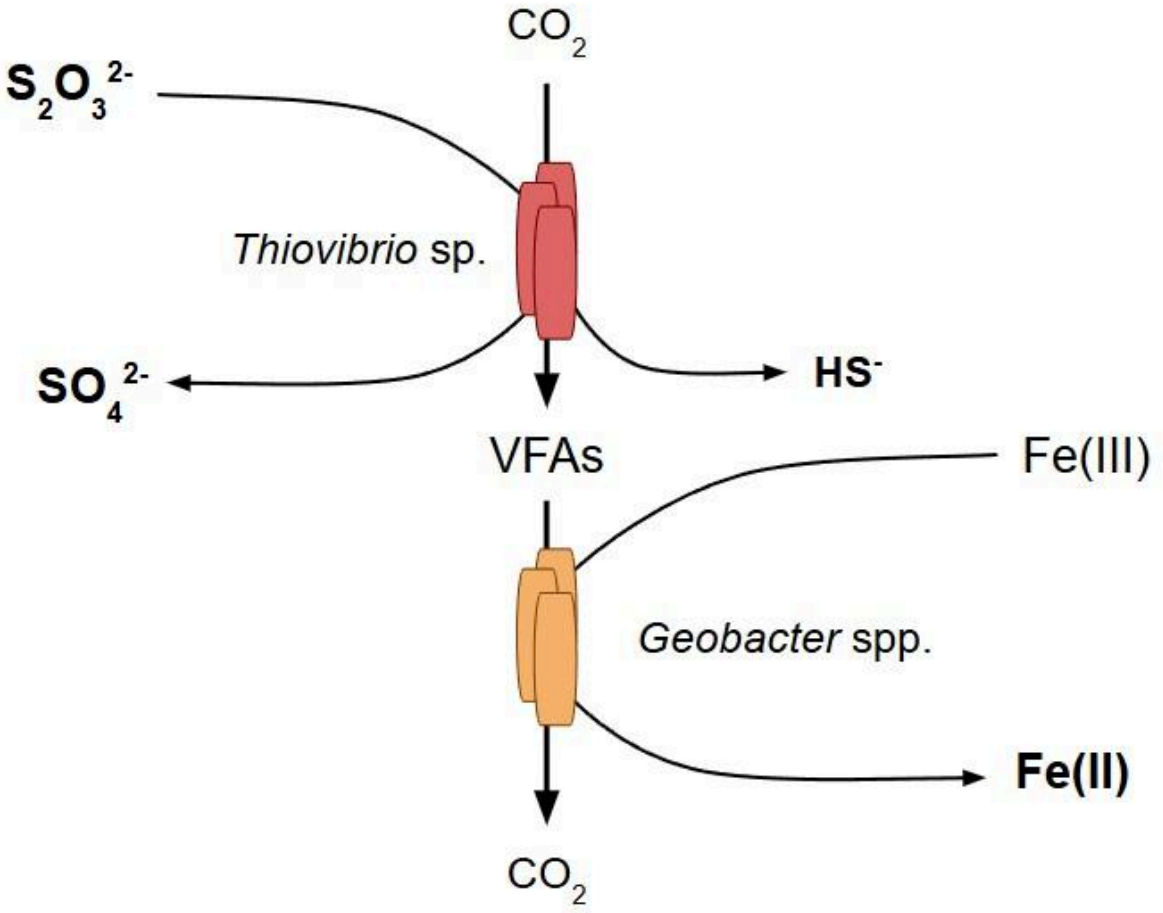

Figure 14. **Proposed 1st model for the interaction of the most relevant species in the thiosulfate oxidation coupled with an iron reduction experiment**. Thiosulfate would be disproportionated in sulfate and sulfide by *Thiovibrio* sp. in order to fix inorganic carbon into VFAs (such lactate and propionate). The VFAs would then be oxidised back to inorganic carbon by *Geobacter* spp. with the coupling of the Fe(III) (ferrihydrite) reduction to Fe(II). Abbreviation: VFAs, Volatile Fatty Acids.

Another possible electron carrier in the redox balance of the experiments is nitrogen (N). The media contain, in fact, NH_4Cl salt that may become a source of ammonia (NH_4^+) for the redox reactions. Has been reported, in fact, that organism of the genera *Geobacter* spp., relevant in our enrichments, are able to couple the oxidation of ammonia with the reduction

of Fe(III) (Equation 25) (Weber et al., 2006; Yang et al., 2012; Rodríguez et al., 2021, Guan et al., 2023).

$$8\ Fe(OH)_3 + NH_4^+ + 14\ H^+ \rightarrow 8\ Fe^{2+} + NO_3^- + H_2O \quad (25)$$

The nearly formed nitrate (NO_3^-) would be then used as an electron acceptor. This is an interesting consideration since the presence in the enrichment of *Trichlorobacter* sp. and *Desulfovibrio* sp., genera reported to be capable of dissimilatory nitrate reduction (De Wever et al., 2000; Greene et al., 2003; Sorokin et al., 2023). Another point worth mentioning is that *Thiovibrio frasassiensis* is able to grow if supplemented with both thiosulfate and nitrate (NO_3^-) (Aronson et al., 2023).

However, interactions between Fe and nitrogen (N) are cryptic in nature, since nitrogen species are highly reactive and short-lived in presence of iron oxide and therefore they may escape the measurements (Kappler et al., 2021).

Considering now the starting experimental question, where we hypothesized the coupling of the thiosulfate oxidation with the reduction of Fe(II), a second possible explanation for our data is that the thiosulfate is indeed completely oxidized to sulfate by Fe(III) or by a generic unidentified electron acceptor. In this case, we would expect a ratio between the concentration of sulfate and thiosulfate approaching 2 (Equation 26). Similarly, the sulfate/thiosulfate ratio observed in our experiments is 1.4, close, but slightly deviating from the theoretical value.

$$S_2O_3^{2-} + EC\ ox + H_2O \rightarrow\ 2\ SO_4^{2-} + EC\ red + 2\ H^+ \quad (26)$$

EC ox = Electron Carrier oxidised

EC red = Electron Carrier reduced

This slight variation could be caused by the presence of the low amount of sulfide. That could be formed as a result of the sulfate reduction by SRB (Sulfate Reducing Bacteria) in the community. The reduction of sulfate to sulfide by SRB would be supported by the presence in the enrichment of known sulfur reducing bacteria such *Desulfosporosinus sp.* and *Desulfovibrio sp.*, that are able to reduce sulfate in wetlands even if present in the community in low relative abundance (Li et al., 2006; Pester et al., 2010; Pecheritsyna et al., 2012; Hausmann et al., 2016; Hausmann et al., 2019). In contrast to our expectation, no *Desulfosporosinus sp.* or *Desulfovibrio sp.* was found above 2 % relative abundance in the thiosulfate only treatment. It is important to note the low relative abundance does not directly disprove this hypothesis, since the abundance of such genera could have been mashed by sampling bias due to the highly abundant *Thiovibrio* sp. or amplification bias derived from the different GC% content of the 16S rRNA gene affecting the amplification steps during the sequencing pipeline (Laursen et al., 2017; Browne et al., 2020).

In this explanation, in the treatment incubated with ferrihydrite and thiosulfate, *Thiovibrio* sp. would indeed couple the thiosulfate oxidation with the ferrihydrite reduction, performing, at the same time, carbon fixation of CO_2 into volatile fatty acids (VFAs). Those compounds could be then used by *Desulfosporosinus* sp. and *Desulfovibrio* sp. in order to reduce sulfate to sulfide, a metabolism well known for this genera (Hines et al., 2001; Duddleston et al., 2002; Li et al., 2006; Hädrich et al., 2012; Hausmann et al., 2016). It must be noted that the total reduced iron recovery may not only be formed by *Thiovibrio* sp. since, in the enrichment

culture, are also present *Geobacter* spp., a genera well known for his ability to breathe Fe(III), as we previously mentioned. This would not overall change the picture as is described, but will imply a higher flux into carbon fixation by the *Thiovibrio* sp. (Figure 15).

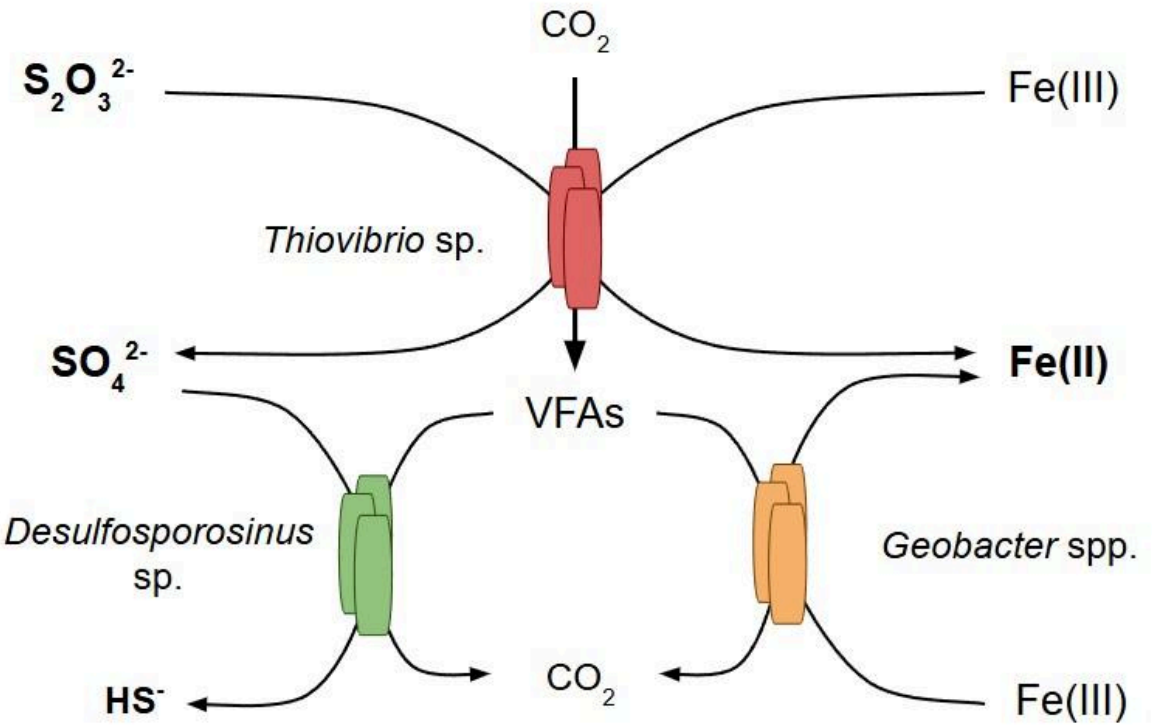

Figure 15. **Proposed 2nd model for the interaction of the most relevant species in the thiosulfate oxidation coupled with an iron reduction experiment**. Thiosulfate would be oxidised in sulfate by *Thiovibrio* sp. in order to fix inorganic carbon into VFAs (such lactate and propionate). The VFAs would then be oxidised back to inorganic carbon by *Desulfosporosinus* sp., coupling the reduction of sulfate in sulfide, or *Geobacter* spp., coupling the reduction of Fe(III) (ferrihydrite) to Fe(II). Abbreviation: VFAs, Volatile Fatty Acids.

Conversely, in the treatment amended only with thiosulfate *Thiovibrio* sp. can not perform carbon fixation solely with the contribution of the thiosulfate oxidation, since the reaction would be thermodynamically unfavorable (Equation 27). An additional oxidant, which has not yet been identified, would be required.

$S_2O_3^{2-} + 4\ H_2O \rightarrow 2\ SO_4^{2-} + 8\ H^+ + 8\ e^-$	$E^o = 0.09$ V	Thauer et al., 1977
$2\ CO_2 + 8\ H^+ + 8\ e^- \rightarrow 2\ CH_2O + 2\ H_2O$	$E^o = -0.43$ V	Thauer et al., 1977
$E_{tot} = (-0.43\ V) - (0.09\ V) = -0.52$ V		(27)

In this case a possibility would be for *Thiovibrio* sp. to possess a metabolic flexibility allowing it to be able to disproportionate thiosulfate in the absence of ferrihydrite while, in the presence of ferrihydrite, couple thiosulfate oxidation and Fe(III) reduction. This possibility

would be supported by the recently observed metabolic versatility of some chemoautotrophic SOB (Sulfur Oxidizing Bacteria) in the anoxic freshwater sediment (Heinze et al., 2023).

In both scenarios, disproportionation and the complete oxidation of thiosulfate followed by the reduction of the sulfate to sulfide, the enrichment culture in the treatment incubated with ferrihydrite and thiosulfate should be able to harvest from various redox reaction free e^-. This net electron would be then used in the synthesis of new biomass by the community as we could see from the results.

This significant increase in the bacterial biomass in the treatments incubated with ferrihydrite and thiosulfate can, in fact, be observed by both the DNA yields and by the microscopy characterization when we compare cell density and DNA yields to the treatments incubated with thiosulfate only, ferrihydrite only or to the treatments without any substrate addition (culture only). Is also interesting to note, that incubation with thiosulfate only, seems not to induce growth in the enrichment culture, as we would expect from the metabolic activities of *Thiovibrio* sp. (Figure 16).

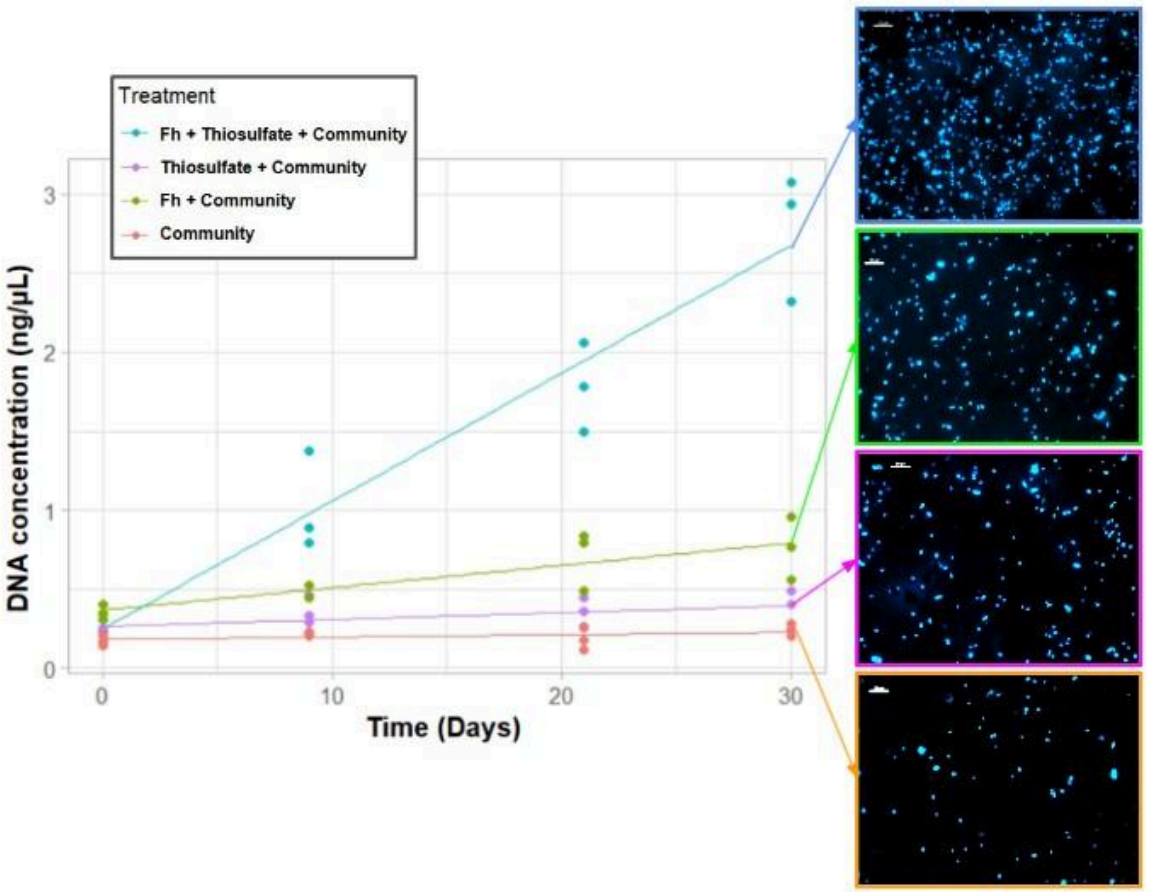

Figure 16. **DNA yields and cell density in the thiosulfate oxidation coupled with an iron reduction experiment**. It could be observed that, only in the enrichment culture provided with thiosulfate and ferrihydrite, an increase in the DNA yields occurs translating in a higher cell density at the 30th days of incubation. Less or no growth is observed in the other treatments if compared with the thiosulfate and ferrihydrite amended treatment.

This could mean that, in order to grow, the enrichment culture needs the presence of several metabolic active species. We could in fact observe the presence, in the treatment incubate with thiosulfate and ferrihydrite, of the key member found in the treatments incubate with thiosulfate only or with ferrihydrite only. In particular, we can notice the presence of *Thiovibrio* sp. from the thiosulfate only incubation, and the presence of *Geobacter* spp., *Desulfovibrio* sp. and *Trichlorobacter* sp. from the ferrihydrite only incubation. In particular for *Geobacter* spp., several studies have been conducted on his ability to grow cooperatively with other species (Cord-Ruwisch et al., 1998; Moscoviz et al., 2017; Wan et al., 2018). And more in general is known that some bacteria growth cooperating with other species (Wintermute and Silver, 2010; Freilich et al., 2011; Pande and Kost, 2017; Smith et al., 2019; Lopes et al., 2024; West and Griffin, 2024).

An alternative possible explanation involves the cytotoxicity of the sulfide (HS^-) for the bacteria (Mirzoyan and Schreier, 2014; Fu et al., 2018). In this possibility the community amended with thiosulfate and ferrihydrite would be able to grow since the HS^- is sequestered, in non-toxic FeS form, by the nearly formed Fe(II). While, on the other hand in the treatment amended with thiosulfate only, without Fe(II), the sulfide accumulates in the media and would be the responsable for the inhibition of the bacterial growth. Must be noted that, based on our results, the inhibition should be constrained only to the cell growth, since the metabolism is active over the entire 30 day incubation period in both treatments.

Conclusion

In conclusion, my results highlight a community capable of coupling thiosulfate oxidation with iron reduction. However, under our experimental conditions, we could not provide unequivocal evidence on how these two reactions are coupled or how this coupling is linked to the growth of the culture.

In our enrichment culture, *Thiovibrio* sp. seems to oxidize the thiosulfate to sulfate, either via iron reduction or via thiosulfate disproportionation. And, at the same time, the culture seems to couple this reaction with the fixation of inorganic carbon in volatile fatty acids (VFAs). Those volatile fatty acids (VFAs) are then oxidised back to inorganic carbon by other members of the community, e.g.,either fueling the reduction of sulfate to sulfide by *Desulfosporosinus* sp., or the reduction of the Fe(III) minerals to Fe(II) by the members of the Geobacteraceae family (*Geobacter* sp. and *Trichlorobacter* sp.).

Another interesting finding is that the enrichment culture seems unable to grow on thiosulfate alone. We would expect for *Thiovibrio* sp. to grow via disproportionation, even without the presence of ferrihydrite. But this didn't seem the case; the culture required ferrihydrite in order to grow. This could be due to several reasons: 1) syntrophic nature of the community, where the microbial consortia are able to grow only if all members are metabolically active; or 2) the toxicity of the sulfide (HS^-). The accumulation of sulfide produced from thiosulfate disproportionation may inhibit the growth of the community. In contrast, ferrihydrite allows to scavenge the toxic sulfide into less toxic FeS, and thereby support the growth.

Those findings are particularly relevant for the understanding of the wetland geochemistry, as they impact the nutrient availability, greenhouse gas emissions, and overall ecosystem function, helping in future studies of biogeochemical modeling and environmental management in wetlands ecosystems.

Acknowledgement

Reference

Abdalla, M., Hastings, A., Truu, J., Espenberg, M., Mander, Ü., & Smith, P. (2016). Emissions of methane from northern peatlands: a review of management impacts and implications for future management options. Ecology and Evolution, 6(19), 7080-7102.

Anantharaman, K., Hausmann, B., Jungbluth, S. P., Kantor, R. S., Lavy, A., Warren, L. A., ... & Banfield, J. F. (2018). Expanded diversity of microbial groups that shape the dissimilatory sulfur cycle. The ISME journal, 12(7), 1715-1728.

Apprill, A., McNally, S., Parsons, R., & Weber, L. (2015). Minor revision to V4 region SSU rRNA 806R gene primer greatly increases detection of SAR11 bacterioplankton. Aquatic Microbial Ecology, 75(2), 129-137.

Aronson, H. S., Thomas, C., Bhattacharyya, M. K., Eckstein, S. R., Jensen, S. R., Barco, R. A., ... & Amend, J. P. (2023). Thiovibrio frasassiensis gen. nov., sp. nov., an autotrophic, elemental sulphur disproportionating bacterium isolated from sulphidic karst sediment, and proposal of Thiovibrionaceae fam. nov. International journal of systematic and evolutionary microbiology, 73(8), 006003.

Bak, F., & Cypionka, H. (1987). A novel type of energy metabolism involving fermentation of inorganic sulphur compounds. Nature, 326(6116), 891-892.

Berg, J. S., Jézéquel, D., Duverger, A., Lamy, D., Laberty-Robert, C., & Miot, J. (2019). Microbial diversity involved in iron and cryptic sulfur cycling in the ferruginous, low-sulfate waters of Lake Pavin. PLoS One, 14(2), e0212787.

Boothroyd, I. M., Worrall, F., Moody, C. S., Clay, G. D., Abbott, G. D., & Rose, R. (2021). Sulfur constraints on the carbon cycle of a blanket bog peatland. Journal of Geophysical Research: Biogeosciences, 126(8), e2021JG006435.

Brock, T. D., & Gustafson, J. O. H. N. (1976). Ferric iron reduction by sulfur-and iron-oxidizing bacteria. Applied and environmental microbiology, 32(4), 567-571.

Browne, P. D., Nielsen, T. K., Kot, W., Aggerholm, A., Gilbert, M. T. P., Puetz, L., ... & Hansen, L. H. (2020). GC bias affects genomic and metagenomic reconstructions, underrepresenting GC-poor organisms. GigaScience, 9(2), giaa008.

Bryce, C., Blackwell, N., Schmidt, C., Otte, J., Huang, Y. M., Kleindienst, S., ... & Kappler, A. (2018). Microbial anaerobic Fe (II) oxidation–ecology, mechanisms and environmental implications. Environmental microbiology, 20(10), 3462-3483.

Caccavo Jr, F., Blakemore, R. P., & Lovley, D. R. (1992). A hydrogen-oxidizing, Fe (III)-reducing microorganism from the Great Bay Estuary, New Hampshire. Applied and Environmental Microbiology, 58(10), 3211-3216.

Caccavo Jr, F., Lonergan, D. J., Lovley, D. R., Davis, M., Stolz, J. F., & McInerney, M. J. (1994). Geobacter sulfurreducens sp. nov., a hydrogen-and acetate-oxidizing dissimilatory metal-reducing microorganism. Applied and environmental microbiology, 60(10), 3752-3759.

Callahan, B. J., McMurdie, P. J., Rosen, M. J., Han, A. W., Johnson, A. J. A., & Holmes, S. P. (2016). DADA2: High-resolution sample inference from Illumina amplicon data. Nature methods, 13(7), 581-583.

Callahan, B. J., Sankaran, K., Fukuyama, J. A., McMurdie, P. J., & Holmes, S. P. (2016). Bioconductor workflow for microbiome data analysis: from raw reads to community analyses. F1000Research, 5.

Canfield, D. E. (2004). The evolution of the Earth surface sulfur reservoir. American Journal of Science, 304(10), 839-861.

Charman, D. J. (2009). Peat and peatlands. Encyclopedia of inland waters, 541-548.

Chen, C., Hall, S. J., Coward, E., & Thompson, A. (2020). Iron-mediated organic matter decomposition in humid soils can counteract protection. Nature communications, 11(1), 2255.

Cline, J. D. (1969). Spectrophotometric determination of hydrogen sulfide in natural waters 1. Limnology and Oceanography, 14(3), 454-458.

Coleman, M. L., Hedrick, D. B., Lovley, D. R., White, D. C., & Pye, K. (1993). Reduction of Fe (III) in sediments by sulphate-reducing bacteria. Nature, 361(6411), 436-438.

Colombo, C., Palumbo, G., He, J. Z., Pinton, R., & Cesco, S. (2014). Review on iron availability in soil: interaction of Fe minerals, plants, and microbes. Journal of soils and sediments, 14, 538-548.

Cord-Ruwisch, R., Lovley, D. R., & Schink, B. (1998). Growth of Geobacter sulfurreducens with acetate in syntrophic cooperation with hydrogen-oxidizing anaerobic partners. Applied and environmental microbiology, 64(6), 2232-2236.

Croal, L. R., Jiao, Y., & Newman, D. K. (2007). The fox operon from Rhodobacter strain SW2 promotes phototrophic Fe (II) oxidation in Rhodobacter capsulatus SB1003. Journal of Bacteriology, 189(5), 1774-1782.

Curtinrich, H. J., Sebestyen, S. D., & Hall, S. J. (2024). Metal-bound carbon and nutrients across hydrologically diverse boreal peatlands. Biogeochemistry, 168(1), 7.

Daugherty, E. E., Gilbert, B., Nico, P. S., & Borch, T. (2017). Complexation and redox buffering of iron (II) by dissolved organic matter. Environmental science & technology, 51(19), 11096-11104.

De Bont, L., Donnay, N., Couturier, J., & Rouhier, N. (2022). Redox regulation of enzymes involved in sulfate assimilation and in the synthesis of sulfur-containing amino acids and glutathione in plants. Frontiers in Plant Science, 13, 958490.

De Wever, H., Cole, J. R., Fettig, M. R., Hogan, D. A., & Tiedje, J. M. (2000). Reductive dehalogenation of trichloroacetic acid by Trichlorobacter thiogenes gen. nov., sp. nov. Applied and environmental microbiology, 66(6), 2297-2301.

Diao, M., Dyksma, S., Koeksoy, E., Ngugi, D. K., Anantharaman, K., Loy, A., & Pester, M. (2023). Global diversity and inferred ecophysiology of microorganisms with the potential for dissimilatory sulfate/sulfite reduction. FEMS Microbiology Reviews, 47(5), fuad058.

Dong, H., Zeng, Q., Sheng, Y., Chen, C., Yu, G., & Kappler, A. (2023). Coupled iron cycling and organic matter transformation across redox interfaces. Nature Reviews Earth & Environment, 4(9), 659-673.

Dos Santos Afonso, M., & Stumm, W. (1992). Reductive dissolution of iron (III)(hydr) oxides by hydrogen sulfide. Langmuir, 8(6), 1671-1675.

Duddleston, K. N., Kinney, M. A., Kiene, R. P., & Hines, M. E. (2002). Anaerobic microbial biogeochemistry in a northern bog: acetate as a dominant metabolic end product. Global Biogeochemical Cycles, 16(4), 11-1.

Emerson, D., & Weiss, J. V. (2004). Bacterial iron oxidation in circumneutral freshwater habitats: findings from the field and the laboratory. Geomicrobiology Journal, 21(6), 405-414.

Emerson, D., Fleming, E. J., & McBeth, J. M. (2010). Iron-oxidizing bacteria: an environmental and genomic perspective. Annual review of microbiology, 64(1), 561-583.

Findlay, A. J., & Kamyshny, A. (2017). Turnover Rates of Intermediate Sulfur Species (S x 2-, S0, S2 O 3 2-, S4 O 6 2-, SO 3 2-) in Anoxic Freshwater and Sediments. Frontiers in Microbiology, 8, 2551.

Finster, K. (2008). Microbiological disproportionation of inorganic sulfur compounds. Journal of Sulfur Chemistry, 29(3-4), 281-292.

Florentino, A. P., Brienza, C., Stams, A. J., & Sanchez-Andrea, I. (2016). Desulfurella amilsii sp. nov., a novel acidotolerant sulfur-respiring bacterium isolated from acidic river sediments. International Journal of Systematic and Evolutionary Microbiology, 66(3), 1249-1253.

Flynn, T. M., O'Loughlin, E. J., Mishra, B., DiChristina, T. J., & Kemner, K. M. (2014). Sulfur-mediated electron shuttling during bacterial iron reduction. Science, 344(6187), 1039-1042.

Freilich, S., Zarecki, R., Eilam, O., Segal, E. S., Henry, C. S., Kupiec, M., ... & Ruppin, E. (2011). Competitive and cooperative metabolic interactions in bacterial communities. Nature communications, 2(1), 589.

Frey, P. A., & Reed, G. H. (2012). The ubiquity of iron.

Fortin, D., & Langley, S. (2005). Formation and occurrence of biogenic iron-rich minerals. Earth-Science Reviews, 72(1-2), 1-19.

Frolking, S., Talbot, J., Jones, M. C., Treat, C. C., Kauffman, J. B., Tuittila, E. S., & Roulet, N. (2011). Peatlands in the Earth's 21st century climate system. Environmental Reviews, 19(NA), 371-396.

Fu, L. H., Wei, Z. Z., Hu, K. D., Hu, L. Y., Li, Y. H., Chen, X. Y., ... & Zhang, H. (2018). Hydrogen sulfide inhibits the growth of Escherichia coli through oxidative damage. journal of microbiology, 56, 238-245.

Gallego-Sala, A. V., Charman, D. J., Brewer, S., Page, S. E., Prentice, I. C., Friedlingstein, P., ... & Zhao, Y. (2018). Latitudinal limits to the predicted increase of the peatland carbon sink with warming. Nature climate change, 8(10), 907-913.

Greene, E. A., Hubert, C., Nemati, M., Jenneman, G. E., & Voordouw, G. (2003). Nitrite reductase activity of sulphate‐reducing bacteria prevents their inhibition by nitrate‐reducing, sulphide‐oxidizing bacteria. Environmental microbiology, 5(7), 607-617.

Guan, Q., Li, T., Zhou, Y., Yang, F., & Li, Q. (2023). Nitrogen loss through anaerobic ammonium oxidation coupled with ferric iron reduction in the Yellow River Wetland, Sanmenxia, China. Limnologica, 102, 126106.

Hädrich, A., Heuer, V. B., Herrmann, M., Hinrichs, K. U., & Küsel, K. (2012). Origin and fate of acetate in an acidic fen. FEMS microbiology ecology, 81(2), 339-354.

Hädrich, A., Taillefert, M., Akob, D. M., Cooper, R. E., Litzba, U., Wagner, F. E., ... & Küsel, K. (2019). Microbial Fe (II) oxidation by Sideroxydans lithotrophicus ES-1 in the presence of Schlöppnerbrunnen fen-derived humic acids. FEMS Microbiology Ecology, 95(4), fiz034.

Hansel, C. M., Lentini, C. J., Tang, Y., Johnston, D. T., Wankel, S. D., & Jardine, P. M. (2015). Dominance of sulfur-fueled iron oxide reduction in low-sulfate freshwater sediments. The ISME journal, 9(11), 2400-2412

Hausmann, B., Knorr, K. H., Schreck, K., Tringe, S. G., Glavina del Rio, T., Loy, A., & Pester, M. (2016). Consortia of low-abundance bacteria drive sulfate reduction-dependent degradation of fermentation products in peat soil microcosms. The ISME Journal, 10(10), 2365-2375.

Hausmann, B., Pjevac, P., Huemer, M., Herbold, C. W., Pester, M., & Loy, A. (2019). Draft genome sequence of Desulfosporosinus sp. strain Sb-LF, isolated from an acidic peatland in Germany. Microbiology Resource Announcements, 8(29), 10-1128.

Heinze, B. M., Küsel, K., Jehmlich, N., von Bergen, M., & Taubert, M. (2023). Metabolic versatility enables sulfur-oxidizers to dominate primary production in groundwater. Water Research, 244, 120426.

Heising, S., Richter, L., Ludwig, W., & Schink, B. (1999). Chlorobium ferrooxidans sp. nov., a phototrophic green sulfur bacterium that oxidizes ferrous iron in coculture with a “Geospirillum” sp. strain. Archives of Microbiology, 172, 116-124.

Herndon, E., AlBashaireh, A., Singer, D., Chowdhury, T. R., Gu, B., & Graham, D. (2017). Influence of iron redox cycling on organo-mineral associations in Arctic tundra soil. Geochimica et Cosmochimica Acta, 207, 210-231.

Hinckley, E. L. S., Crawford, J. T., Fakhraei, H., & Driscoll, C. T. (2020). A shift in sulfur-cycle manipulation from atmospheric emissions to agricultural additions. Nature Geoscience, 13(9), 597-604.

Holmer, M., & Storkholm, P. (2001). Sulphate reduction and sulphur cycling in lake sediments: a review. Freshwater Biology, 46(4), 431-451.

Hori, T., Aoyagi, T., Itoh, H., Narihiro, T., Oikawa, A., Suzuki, K., ... & Kamagata, Y. (2015). Isolation of microorganisms involved in reduction of crystalline iron (III) oxides in natural environments. Frontiers in Microbiology, 6, 386.

Huang, S., & Jaffé, P. R. (2018). Isolation and characterization of an ammonium-oxidizing iron reducer: Acidimicrobiaceae sp. A6. PLoS One, 13(4), e0194007.

Ionescu, D., Heim, C., Polerecky, L., Thiel, V., & De Beer, D. (2015). Biotic and abiotic oxidation and reduction of iron at circumneutral pH are inseparable processes under natural conditions. Geomicrobiology Journal, 32(3-4), 221-230.

Jackson, B. E., & McInerney, M. J. (2000). Thiosulfate disproportionation by Desulfotomaculum thermobenzoicum. Applied and Environmental Microbiology, 66(8), 3650-3653.

Jaszczuk, I., Jabłońska, E., Kozub, Ł., Tanneberger, F., Aggenbach, C., Seeber, E., ... & Kotowski, W. (2024). Peat formation potential of temperate fens increases with hydrological stability. Science of the Total Environment, 947, 174617.

Jiao, Y., Kappler, A., Croal, L. R., & Newman, D. K. (2005). Isolation and characterization of a genetically tractable photoautotrophic Fe (II)-oxidizing bacterium, Rhodopseudomonas palustris strain TIE-1. Applied and Environmental Microbiology, 71(8), 4487-4496.

Jørgensen, B. B. (1990). The sulfur cycle of freshwater sediments: role of thiosulfate. Limnology and Oceanography, 35(6), 1329-1342.

Kappler, A., & Newman, D. K. (2004). Formation of Fe (III)-minerals by Fe (II)-oxidizing photoautotrophic bacteria. Geochimica et Cosmochimica Acta, 68(6), 1217-1226.

Kappler, A., Bryce, C., Mansor, M., Lueder, U., Byrne, J. M., & Swanner, E. D. (2021). An evolving view on biogeochemical cycling of iron. Nature Reviews Microbiology, 19(6), 360-374.

Katoh, K., Misawa, K., Kuma, K. I., & Miyata, T. (2002). MAFFT: a novel method for rapid multiple sequence alignment based on fast Fourier transform. Nucleic acids research, 30(14), 3059-3066.

Knorr, K. H. (2013). DOC-dynamics in a small headwater catchment as driven by redox fluctuations and hydrological flow paths–are DOC exports mediated by iron reduction/oxidation cycles?. Biogeosciences, 10(2), 891-904.

Kügler, S., Cooper, R. E., Wegner, C. E., Mohr, J. F., Wichard, T., & Küsel, K. (2019). Iron-organic matter complexes accelerate microbial iron cycling in an iron-rich fen. Science of the total environment, 646, 972-988.

Küsel, K., Blöthe, M., Schulz, D., Reiche, M., & Drake, H. L. (2008). Microbial reduction of iron and porewater biogeochemistry in acidic peatlands. Biogeosciences, 5(6), 1537-1549.

Kwon, M. J., Boyanov, M. I., Antonopoulos, D. A., Brulc, J. M., Johnston, E. R., Skinner, K. A., ... & O'Loughlin, E. J. (2014). Effects of dissimilatory sulfate reduction on FeIII (hydr) oxide reduction and microbial community development. Geochimica et Cosmochimica Acta, 129, 177-190.

Laursen, M. F., Dalgaard, M. D., & Bahl, M. I. (2017). Genomic GC-content affects the accuracy of 16S rRNA gene sequencing based microbial profiling due to PCR bias. Frontiers in microbiology, 8, 1934.

Leifeld, J., & Menichetti, L. (2018). The underappreciated potential of peatlands in global climate change mitigation strategies. Nature communications, 9(1), 1071.

Lensmire, J. M., & Hammer, N. D. (2019). Nutrient sulfur acquisition strategies employed by bacterial pathogens. Current opinion in microbiology, 47, 52-58.

Li, Y. L., Vali, H., Yang, J., Phelps, T. J., & Zhang, C. L. (2006). Reduction of iron oxides enhanced by a sulfate-reducing bacterium and biogenic H2S. Geomicrobiology Journal, 23(2), 103-117.

Li, Q., Hu, W., Li, L., & Li, Y. (2023). Interactions between organic matter and Fe oxides at soil micro-interfaces: Quantification, associations, and influencing factors. Science of the Total Environment, 855, 158710.

Liamleam, W., & Annachhatre, A. P. (2007). Electron donors for biological sulfate reduction. Biotechnology advances, 25(5), 452-463.

Limpens, J., Berendse, F., Blodau, C., Canadell, J. G., Freeman, C., Holden, J., ... & Schaepman-Strub, G. (2008). Peatlands and the carbon cycle: from local processes to global implications–a synthesis. Biogeosciences, 5(5), 1475-1491.

Lin, S., Mackey, H. R., Hao, T., Guo, G., Van Loosdrecht, M. C., & Chen, G. (2018). Biological sulfur oxidation in wastewater treatment: a review of emerging opportunities. Water research, 143, 399-415.

Lin, F., Zuo, H., Ma, X., & Ma, L. (2022). Comprehensive assessment of nitrous oxide emissions and mitigation potentials across European peatlands. Environmental Pollution, 301, 119041.

Liu, L., Zheng, N., Yu, Y., Zheng, Z., & Yao, H. (2024). Soil carbon and nitrogen cycles driven by iron redox: A review. Science of The Total Environment, 170660.

Lopes, W., Amor, D. R., & Gore, J. (2024). Cooperative growth in microbial communities is a driver of multistability. Nature Communications, 15(1), 4709.

Lovley, D. R., & Phillips, E. J. (1988). Novel mode of microbial energy metabolism: organic carbon oxidation coupled to dissimilatory reduction of iron or manganese. Applied and environmental microbiology, 54(6), 1472-1480.

Lovley, D. R., Phillips, E. J., & Caccavo Jr, F. (1992). Acetate oxidation by dissimilatory Fe (III) reducers. Applied and Environmental Microbiology, 58(9), 3205-3208.

Lovley, D. R., Holmes, D. E., & Nevin, K. P. (2004). Dissimilatory fe (iii) and mn (iv) reduction. Advances in microbial physiology, 49(2), 219-286.

Melton, E. D., Schmidt, C., & Kappler, A. (2012). Microbial iron (II) oxidation in littoral freshwater lake sediment: the potential for competition between phototrophic vs. nitrate-reducing iron (II)-oxidizers. Frontiers in microbiology, 3, 197.

Mirzoyan, N., & Schreier, H. J. (2014). Effect of sulfide on growth of marine bacteria. Archives of microbiology, 196(4), 279-287.

Moscoviz, R., de Fouchécour, F., Santa-Catalina, G., Bernet, N., & Trably, E. (2017). Cooperative growth of Geobacter sulfurreducens and Clostridium pasteurianum with subsequent metabolic shift in glycerol fermentation. Scientific reports, 7(1), 44334.

Muyzer, G., & Stams, A. J. (2008). The ecology and biotechnology of sulphate-reducing bacteria. Nature reviews microbiology, 6(6), 441-454.

Myers, C. R., & Nealson, K. H. (1990). Respiration-linked proton translocation coupled to anaerobic reduction of manganese (IV) and iron (III) in Shewanella putrefaciens MR-1. Journal of Bacteriology, 172(11), 6232-6238.

Pande, S., & Kost, C. (2017). Bacterial unculturability and the formation of intercellular metabolic networks. Trends in microbiology, 25(5), 349-361.

Parada, A. E., Needham, D. M., & Fuhrman, J. A. (2016). Every base matters: assessing small subunit rRNA primers for marine microbiomes with mock communities, time series and global field samples. Environmental microbiology, 18(5), 1403-1414.

Pecheritsyna, S. A., Rivkina, E. M., Akimov, V. N., & Shcherbakova, V. A. (2012). Desulfovibrio arcticus sp. nov., a psychrotolerant sulfate-reducing bacterium from a cryopeg. International journal of systematic and evolutionary microbiology, 62(1), 33-37.

Peduzzi, S., Tonolla, M., & Hahn, D. (2003). Isolation and characterization of aggregate-forming sulfate-reducing and purple sulfur bacteria from the chemocline of meromictic Lake Cadagno, Switzerland. FEMS microbiology ecology, 45(1), 29-37.

Pester, M., Bittner, N., Deevong, P., Wagner, M., & Loy, A. (2010). A ‘rare biosphere’microorganism contributes to sulfate reduction in a peatland. The ISME journal, 4(12), 1591-1602.

Pjevac, P., Hausmann, B., Schwarz, J., Kohl, G., Herbold, C. W., Loy, A., & Berry, D. (2021). An economical and flexible dual barcoding, two-step PCR approach for highly multiplexed amplicon sequencing. Frontiers in microbiology, 12, 669776.

R Core Team. (2013). R: A language and environment for statistical computing. Foundation for Statistical Computing, Vienna, Austria.

Roden, E. E. (2006). Geochemical and microbiological controls on dissimilatory iron reduction. Comptes rendus. Géoscience, 338(6-7), 456-467.

Rodhe, H. (1999). Human impact on the atmospheric sulfur balance. Tellus B, 51(1), 110-122.

Rodríguez, C., Cisternas, J., Serrano, J., & Leiva, E. (2021). Nitrogen removal by an anaerobic iron-dependent ammonium oxidation (Feammox) enrichment: Potential for wastewater treatment. Water, 13(23), 3462.

Rue, E. L., & Bruland, K. W. (1995). Complexation of iron (III) by natural organic ligands in the Central North Pacific as determined by a new competitive ligand equilibration/adsorptive cathodic stripping voltammetric method. Marine chemistry, 50(1-4), 117-138.

Sivan, O., Adler, M., Pearson, A., Gelman, F., Bar-Or, I., John, S. G., & Eckert, W. (2011). Geochemical evidence for iron-mediated anaerobic oxidation of methane. Limnology and Oceanography, 56(4), 1536-1544.

Slobodkin, A. I., & Slobodkina, G. B. (2019). Diversity of sulfur-disproportionating microorganisms. Microbiology, 88, 509-522.

Smith, N. W., Shorten, P. R., Altermann, E., Roy, N. C., & McNabb, W. C. (2019). The classification and evolution of bacterial cross-feeding. Frontiers in Ecology and Evolution, 7, 153.

Song, X., Wang, P., Van Zwieten, L., Bolan, N., Wang, H., Li, X., ... & Li, F. (2022). Towards a better understanding of the role of Fe cycling in soil for carbon stabilization and degradation. Carbon Research, 1(1), 5.

Sorokin, D. Y., Tikhonova, T. V., Koch, H., van den Berg, E. M., Hinderks, R. S., Pabst, M., ... & Lücker, S. (2023). Trichlorobacter ammonificans, a dedicated acetate-dependent ammonifier with a novel module for dissimilatory nitrate reduction to ammonia. The ISME Journal, 17(10), 1639-1648.

Straub, K. L., Benz, M., Schink, B., & Widdel, F. (1996). Anaerobic, nitrate-dependent microbial oxidation of ferrous iron. Applied and environmental microbiology, 62(4), 1458-1460.

Straub, K. L., Benz, M., & Schink, B. (2001). Iron metabolism in anoxic environments at near neutral pH. FEMS microbiology ecology, 34(3), 181-186.

Sulzberger, B. (2015). Light-induced redox cycling of iron: roles for CO 2 uptake and release by aquatic ecosystems. Aquatic geochemistry, 21, 65-80.

Thamdrup, B. O., Finster, K., Hansen, J. W., & Bak, F. (1993). Bacterial disproportionation of elemental sulfur coupled to chemical reduction of iron or manganese. Applied and environmental microbiology, 59(1), 101-108.

Thauer, R. K., Jungermann, K., & Decker, K. (1977). Energy conservation in chemotrophic anaerobic bacteria. Bacteriological reviews, 41(1), 100-180.

Wan, Y., Zhou, L., Wang, S., Liao, C., Li, N., Liu, W., & Wang, X. (2018). Syntrophic growth of Geobacter sulfurreducens accelerates anaerobic denitrification. Frontiers in Microbiology, 9, 1572.

Wasmund, K., Mußmann, M., & Loy, A. (2017). The life sulfuric: microbial ecology of sulfur cycling in marine sediments. Environmental microbiology reports, 9(4), 323-344.

Wayne, W. (1988). [27] Rapid colorimetric micromethod for the quantitation of complexed iron in biological samples. In Methods in enzymology (Vol. 158, pp. 357-364). Academic Press.

Weber, K. A., Achenbach, L. A., & Coates, J. D. (2006). Microorganisms pumping iron: anaerobic microbial iron oxidation and reduction. Nature Reviews Microbiology, 4(10), 752-764.

Weber, K. A., Urrutia, M. M., Churchill, P. F., Kukkadapu, R. K., & Roden, E. E. (2006). Anaerobic redox cycling of iron by freshwater sediment microorganisms. Environmental Microbiology, 8(1), 100-113.

Wei, C., Yin, S., Kappler, A., Tao, S., & Zhu, D. (2023). A new pathway for pyrite formation in low-sulfate sediments driven by mineralization of reduced organic sulfur. Fundamental Research.

West, S. A., & Griffin, A. S. (2024). Microbial primer: cooperation in bacteria. Microbiology, 170(4), 001440.

Widdel, F., Schnell, S., Heising, S., Ehrenreich, A., Assmus, B., & Schink, B. (1993). Ferrous iron oxidation by anoxygenic phototrophic bacteria. Nature, 362(6423), 834-836.

Wintermute, E. H., & Silver, P. A. (2010). Emergent cooperation in microbial metabolism. Molecular systems biology, 6(1), 407.

Wu, B., Liu, F., Fang, W., Yang, T., Chen, G. H., He, Z., & Wang, S. (2021). Microbial sulfur metabolism and environmental implications. Science of The Total Environment, 778, 146085.

Yang, W. H., Weber, K. A., & Silver, W. L. (2012). Nitrogen loss from soil through anaerobic ammonium oxidation coupled to iron reduction. Nature Geoscience, 5(8), 538-541.

Yang, L., Jiang, M., Zou, Y., Qin, L., & Chen, Y. (2021). Geographical distribution of iron redox cycling bacterial community in peatlands: distinct assemble mechanism across environmental gradient. Frontiers in Microbiology, 12, 674411.

Yu, Z., Loisel, J., Brosseau, D. P., Beilman, D. W., & Hunt, S. J. (2010). Global peatland dynamics since the Last Glacial Maximum. Geophysical research letters, 37(13).

Yu, Z. C. (2012). Northern peatland carbon stocks and dynamics: a review. Biogeosciences, 9(10), 4071-4085.

Zak, D., Hupfer, M., Cabezas, A., Jurasinski, G., Audet, J., Kleeberg, A., ... & Goldhammer, T. (2021). Sulphate in freshwater ecosystems: A review of sources, biogeochemical cycles, ecotoxicological effects and bioremediation. Earth-Science Reviews, 212, 103446.

Zhao, Q., & Lu, Y. (2023). Anaerobic oxidation of methane in terrestrial wetlands: The rate, identity and metabolism. Science of the Total Environment, 166049.

Zhou, G. W., Yang, X. R., Li, H., Marshall, C. W., Zheng, B. X., Yan, Y., ... & Zhu, Y. G. (2016). Electron shuttles enhance anaerobic ammonium oxidation coupled to iron (III) reduction. Environmental Science & Technology, 50(17), 9298-9307.

Zhou, Z., Tran, P. Q., Cowley, E. S., Trembath-Reichert, E., & Anantharaman, K. (2024). Diversity and ecology of microbial sulfur metabolism. Nature Reviews Microbiology, 1-19.